New Distribution and Molecular Diversity of the Reniform Nematode *Rotylenchulus macrosoma* Dasgupta, Raski and Sher, 1968 (Nematoda: Rotylenchulinae) in Europe

Juan E. Palomares-Rius[1], Antonio Archidona-Yuste[2], Carolina Cantalapiedra-Navarrete[1], Andrea S. Azpilicueta[3], Antonio Saborido[4], Emmanuel A. Tzortzakakis[5], Ruihang Cai[1,6] and Pablo Castillo[1]

[1]Institute for Sustainable Agriculture (IAS), Spanish National Research Council (CSIC), Avenida Menéndez Pidal s/n, 14004 Córdoba, Campus de Excelencia Internacional Agroalimentario, ceiA3, Spain
[2]Department of Ecological Modelling, Helmholtz Centre for Environmental Research - UFZ, Permoserstrasse 15, 04318 Leipzig, Germany
[3]Cambrico Biotech S. L., C/ Tecnología nº 26 Planta 2. Módulo 1, 41015, Sevilla, Spain
[4]Bayer Crop Science, Avda. Baix Llobregat, 3-5. 08970 Sant Joan Despi, Barcelona, Spain
[5]Institute of Olive Tree, Subtropical Crops and Viticulture, Department of Viticulture, Vegetable Crops, Floriculture and Plant Protection, N.AG.RE.F., Hellenic Agricultural Organization-DEMETER, 32A Kastorias street, Mesa Katsabas, 71307, Heraklion, Crete, Greece
[6]Laboratory of Plant Nematology, Institute of Biotechnology, College of Agriculture and Biotechnology, Zhejiang University, Hangzhou 310058, Zhejiang, P.R. China

Received: _____/Accepted _____.

Corresponding author: Pablo Castillo; E-mail: p.castillo@csic.es

Funding: Financial support was provided by grant 201740E042, "Análisis de diversidad molecular, barcoding, y relaciones filogenéticas de nematodos fitoparásitos en cultivos mediterráneos" from the Spanish National Research Council (CSIC), and RTI2018-095925-A-100 from Ministerio de Ciencia, Innovación y Universidades, Spain.

*The *e*-Xtra logo stands for "electronic extra" and indicates that 6 supplementary figures and 3 tables are published online.

The authors declare no conflicts of interest.

ABSTRACT

Reniform nematodes of the genus *Rotylenchulus* are semiendoparasites of numerous herbaceous and woody plant species roots and occur largely in regions with temperate, subtropical and tropical climates. In this study, we provide new records of the nematode *R. macrosoma* in eight European countries (Czech Republic, France, Germany, Hungary, Italy, Romania, Serbia and Portugal), in addition to the six Mediterranean countries (Greece, Israel, Jordan, Spain, Syria, and Turkey) where the nematode had previously been reported. Four new host species (corn, pea, wheat and an almond-peach hybrid rootstock) are added to the recorded host species (bean, chickpea, hazelnut, peanut, soybean, wild and cultivated olive). Molecular analyses based on the *coxI* and D2-D3 segments of 28S RNA markers showed high diversity and pronounced genetic structure among populations of *R. macrosoma*. However, the complexity of phylogeographic patterns in plant-parasitic nematodes may be related to the intrinsic heterogeneity in the distribution of soil organisms, a rare occurrence of a species, or the potential human impact associated with agricultural practices.

Keywords: reniform nematodes, 28S rDNA D2-D3, *coxI*, phylogeny, taxonomy.

Reniform nematodes of the genus *Rotylenchulus* Linford and Oliveira 1940 are semiendoparasites of numerous wild and cultivated plant species (Fig. 1). The genus comprises 11 species (Van den Berg et al. 2016), which have been reported in 54 countries in Africa, Asia, Australia, Europe, and North and South America (Robinson et al. 1997). The species are distributed mainly in regions with a tropical or warm temperate climate. The life cycle of *Rotylenchulus* nematodes begins with a first molt within the egg, with the second-stage juveniles (J2) hatching from the eggs. Males and juveniles (from J2 to preadult fourth-stage, J4) are found in the soil (Robinson 2007). Immature vermiform females penetrate root tissues and produce different types of feeding sites (a single, giant uninucleate cell or syncytium, depending on the nematode species - host plant combination). Once the root is penetrated, nematodes become sedentary, keeping the anterior portion of their body embedded in the root while the enlarged posterior region protrudes from the root surface (Palomares-Rius et al. 2017; van den Berg et al. 2012). Mature females lay approximately 50 to 60 eggs in a gelatinous matrix that they secrete, forming an external egg mass on the root. *Rotylenchulus* species are characterized by sexual dimorphism; mature females swell to form a kidney shape, and males are vermiform with a less-developed stylet and pharynx as they do not feed (Dasgupta et al. 1968; van den Berg et al. 2012) (Fig. 1). *Rotylenchulus reniformis* Linford and Oliveira 1940 is the most economically important and most widely distributed of the *Rotylenchulus* species; it is a serious soil inhabiting pathogen of cotton (*Gossypium hirsutum* and *G. barbadense*) and other crops in 30 countries in North and South America, Africa, Asia, and Europe (Robinson et al. 1997). In contrast, *R. parvus* (Williams 1960) Sher 1961, and *R. macrosoma* Dasgupta, Raski and Sher 1968, among other species, exhibit a limited distribution and are of less economic importance (Gaur and Perry 1991; Robinson et al. 1997). *Rotylenchulus macrosoma* has been reported in the Mediterranean region in Greece, Israel, Jordan, Spain, Syria, and Turkey (Robinson et al. 1997; Palomares-Rius et al. 2018), but no research has been conducted to explore whether *R. macrosoma* occurs in other countries or regions. *Rotylenchulus macrosoma* has been reported infecting several host plant species, including wild and cultivated olive (*Olea europaea* subs. *sylvestris* and *O. europaea* subs. *europaea*), bean (*Phaseolus vulgaris*), chickpea (*Cicer arietinum*), hazelnut (*Corylus avellana*), peanut (*Arachis hypogaea*), and soybean (*Glycine max*) (Dasgupta et al. 1968; Cohn and Mordechai 1988; Robinson et al. 1997, Sikora et al. 2018). Notably, the phytopathological range of species in this group of nematodes is changing, considering the recent expansion in range of *R. reniformis* to subtropical cotton production areas in Spain

90 (Palomares-Rius et al. 2018; Castillo and Gómez-Barcina 1993; Artero et al. 1977) and the
91 emergence of the species as a problem to cotton production in the USA (Robinson 2007).
92 The biology of *R. reniformis* and other reniform nematodes confer several competitive
93 advantages over other phytopathogenic nematodes including *Meloidogyne* spp. Reniform
94 nematodes (1) survive in dry soil in vermiform stages as an anhydrobiotic form; (2) have
95 shorter life cycles; (3) induce less damage in root tissue, and establish feeding sites along
96 primary, secondary, and tertiary roots, allowing survival at greater depths in the soil; (4) have
97 effective protection against pathogens and predators due to retention of body cuticles (J2 to
98 J4 individuals are not parasitic and retain the cuticles of the previous stages after molting);
99 and (5) have wide ecological adaptation to different soil types (Gaur and Perry 1991; Robinson
100 2007). However, other factors, including their low population density in soil, the lack of
101 apparent impact on some crop yields and the difficulties in accurate identification of some
102 plant-parasitic nematodes (PPN) could restrict the precise determination of the geographical
103 distribution of reniform nematode species. Thus, *Rotylenchulus* spp. may be "neglected" as
104 plant-host damaging pathogens, particularly when considered under projected global climate
105 change scenarios (IPCC 2019). Consequently, it is important to determine the current
106 distribution and adaptation of *Rotylenchulus* spp. to different crop species and environmental
107 conditions to develop and anticipate appropriate management solutions.
108 The genus *Rotylenchulus* has ribosomal RNA (rRNA) genes that exhibit high levels of
109 intraspecific and intra-individual variation (Van Den Berg et al. 2016; Palomares-Rius et al.
110 2018; Qing et al. 2019). The majority of the D2 region types of 28S rRNA (type A and B) in
111 *R. reniformis* have been characterized as functional through the reconstruction of secondary
112 structure models and mutation mapping (Van den Berg et al. 2016). These different sequences
113 are paralogs that are located in different rRNA clusters or chromosomes and the number of
114 tandem arrays may still be expanding (Qing et al. 2019). Additionally, the size of the *R.*
115 *reniformis* genome, based on flow cytometry, is estimated to be 190 Mb which is two to four
116 times larger than the genome of *Caenorhabditis elegans* or the root-knot nematode
117 *Meloidogyne incognita*, respectively (Ganji et al. 2013). Several genomes of *R. reniformis*
118 have been published recently (Nyaku et al. 2014; Showmaker et al. 2019), the most recent
119 having a size of 314 Mb, possibly as a result of unresolved haplotypes derived from
120 heterogeneity within the *R. reniformis* population used for DNA extraction (Showmaker et al.
121 2019). The complete mtDNA sequence has been deposited in GenBank (accession
122 CM003310) and has a length of 24,572 bp, but the annotation of putative gene regions has not
123 been performed.

124 *Rotylenchulus* spp. show high intraspecific variability of some morphological
125 diagnostic features of immature females (the development stage usually employed for species
126 identification) (Van Den Berg et al. 2016), and for this reason, it is necessary to use molecular
127 markers for species identification. In this regard, the use of rRNA markers is challenging due
128 to the previously noted presence of several gene copies that are not well homogenized in the
129 genome, so several different amplicon sizes and associated sequences can be observed
130 following the specific amplification of rRNA genes (Van Den Berg et al. 2016; Palomares-
131 Rius et al. 2018; Qing et al. 2019). A high level of genetic diversity between *R. reniformis*
132 populations from several states in the USA and Japan has been found using microsatellites
133 (Arias et al. 2009; Leach et al. 2012). However, for other species of this genus, the available
134 information is scarce and is based only on rRNA markers. Microsatellites of *R. reniformis*
135 obtained by Leach et al. (2012) did not amplify DNA from samples of *R. macrosoma*
136 (Palomares-Rius, *unpublished*). However, the mitochondrial cytochrome c oxidase subunit 1
137 (*coxI*) sequence has been useful for studying population genetics of other nematode species
138 (Derycke et al. 2008; Gutiérrez-Gutiérrez et al. 2011; Subbotin et al. 2018; Xu et al. 2020).
139 Thus, we used the *coxI* gene in combination with rRNA for population genetic analyses of *R.*
140 *macrosoma* populations.

141 Based on existing information, the distribution of *R. macrosoma* is limited in the
142 Mediterranean Basin (Palomares-Rius et al. 2018). However, we hypothesise the species is
143 more widespread, due to recent range expansion, resulting in a wider distribution with
144 concomitant infection of new host species, as demonstrated with other species of the genus
145 (Palomares-Rius et al. 2018; Castillo and Gómez-Barcina 1993; Artero et al. 1977).
146 Furthermore, we hypothesise that the current phylogenetic pattern of *R. macrosoma* might
147 reflect ancient geographic distributions and climate change (Hewitt 2001; Gomez and Lunt
148 2006). To test these hypotheses, we (1) explored the distribution of *R. macrosoma* in new
149 areas in Europe and the associations of the nematode with new crop species including corn
150 (*Zea mais*) and wheat (*Triticum aestivum*); (2) studied putative species diversity using
151 sequence-based species delimitation methods to objectively interpret *Rotylenchulus* spp.
152 boundaries in the populations that were sampled; and (3) investigated genetic relatedness
153 among populations of *R. macrosoma*.

154

155 **MATERIALS AND METHODS**

156

157 **Nematode population sampling, extraction and morphological identification.** The
158 samples were not collected using a formal survey strategy, but several type of samples
159 containing *R. macrosoma* were obtained, including samples from: 1) previously sampled
160 populations (Palomares-Rius et al. 2018); 2) the nematological identification service
161 laboratory of the Institute for Sustainable Agriculture of the Spanish National Research
162 Council (IAS-CSIC Nematology Laboratory, Cordoba, Spain) that were collected from
163 different crop species at different locations in Europe; and 3) samples collected arbitrarily by
164 the authors from various locations (Table 1). Nematode populations from corn and wheat
165 crops were extracted from soil samples provided by farmers to the IAS-CSIC Nematology
166 Laboratory.

167 A standardized method was used to collect approximately 1.0 kg soil samples from
168 each population. Soil samples were collected with a mattock and a soil tube (40 mm diam.)
169 from 10 to 40 cm depths depending on soil conditions. Soil was collected from the rhizosphere
170 of three to five plants selected in each field, which comprised the 1.0 kg sample. Nematode
171 specimens were extracted from a 500 cm^3 soil sample using the centrifugal flotation method
172 (Coolen 1979). Samples were examined for nematodes using a Leica DM6 compound
173 microscope under differential interference contrast conditions at magnifications up to 1,000x,
174 and a Leica DFC7000 T digital camera was used to capture images of the nematodes.
175 Nematodes were identified to species using an integrative approach combining molecular and
176 morphological techniques to achieve efficient and accurate identification (Palomares-Rius et
177 al. 2018). For each nematode population, key diagnostic characters were determined,
178 including body length, stylet length, a ratio (body length/maximum body width) c' ratio (tail
179 length/body width at anus), V ratio ((distance from anterior end to vulva/body length) × 100),
180 and o ratio ((distance from stylet base to dorsal pharyngeal opening/body length) × 100)
181 (Palomares-Rius et al. 2018) and the sequencing of specific DNA fragments (described below)
182 confirmed the identity of the nematode species for each population. Nematode population
183 density in the soil was assessed as the total number of adult and juvenile-stage individuals in
184 each soil sample.

185

186 **DNA extraction, PCR and sequencing of *coxI* and *D2-D3* sequences.** Juveniles or adults
187 were used for molecular identification and molecular characterization. Nematode DNA was
188 extracted from single individuals as described by Subbotin et al. (2000). PCR and sequencing
189 were performed at the IAS-CSIC facility. The *coxI* gene was amplified using the primers JB3
190 (5′-TTTTTTGGGCATCCTGAGGTTTAT-3′) and JB5 (5′-

191 AGCACCTAAACTTAAAACATAATGAAAATG-3′) (Bowles et al. 1992). For individuals
192 with different haplotypes and those obtained from different populations, the 28S rRNA
193 fragment was also sequenced. The D2-D3 expansion segments of the 28S rRNA gene were
194 amplified using the D2A (5'-ACAAGTACCGTGAGGGAAAGTTG-3') and D3B (5'-
195 TCGGAAGGAACCAGCTACTA-3') primers (De Ley et al. 1999).
196 The PCR cycling conditions for the 28S rRNA primers were as follows: 94 °C for 2
197 min, followed by 35 cycles of 94 °C for 30 s, an annealing temperature of 55 °C for 45 s, and
198 72 °C for 1 min, and one final cycle of 72 °C for 10 min. The PCR cycling for *coxI* primers
199 was as follows: 95 °C for 15 min, 39 cycles at 94 °C for 30 s, 53 °C for 30 s, and 68 °C for 1
200 min, followed by a final extension at 72 °C for 7 min. PCR volumes were adapted to 25 µl for
201 each reaction and primer concentrations were as described in De Ley et al. (1999) and Bowles
202 et al. (1992). 5x HOT FIREpol® Blend Master Mix (Solis Biodyne, Tartu, Estonia) was used
203 in all PCR reactions. The PCR products were purified after amplification using ExoSAP-IT
204 (Affimetrix, USB products, Kandel, Germany), and used for direct sequencing in both
205 directions with the corresponding primers. The resulting products were purified and run in a
206 DNA multicapillary sequencer (Model 3130XL Genetic Analyzer; Applied Biosystems,
207 Foster City, CA, USA), using the BigDye Terminator Sequencing Kit v.3.1 (Applied
208 Biosystems), at the Stab Vida sequencing facility (Caparica, Portugal). The sequence
209 chromatograms of the two markers (*coxI* and D2-D3 expansion segments of 28S rRNA) were
210 analyzed using DNASTAR LASERGENE SeqMan v. 7.1.0. The newly obtained bidirectional
211 sequences were submitted to the National Center for Biotechnology Information (NCBI,
212 Bethesda, MD) GenBank database under the accession numbers indicated in Table 1.
213
214 **Data analyses and population genetic structure.** Sequences from the two markers were
215 aligned separately using ClustalW. The number of sequences and sampling points are
216 presented (Table 1). *coxI* sequences were translated to amino acid sequences before alignment
217 to check for the presence of stop codons using the Alternative Flatworm Mitochondrial Code
218 (transl_table=14) genetic code from NCBI
219 (https://www.ncbi.nlm.nih.gov/Taxonomy/Utils/wprintgc.cgi?mode=c#SG14). However,
220 some haplotypes presented stop codons (TAG) in this region, but their amino acid sequence
221 corresponded to the COXI protein. The nucleotide substitution map for the *coxI* region was
222 calculated with the package *adegenet* (Jombart 2008) in R v. 3.5.1 (R Core Team 2019).
223 Genetic diversity within sampling sites was investigated by calculating nucleotide diversity
224 (π) and haplotype diversity (h) using DNA Sequence Polymorphism software (DnaSP) v. 6

225 (Rozas et al. 2017) according to Nei (1987). To investigate whether sequence evolution
226 followed a neutral model, Tajima's D and Fu's Fs neutrality tests were performed. The two
227 tests are used to gauge whether the populations had experienced expansion (Rogers and
228 Harpending 1992). This is an important aspect of the populations to understand since reniform
229 nematodes are assumed to be distributed in warmer temperate and tropical climates, rather
230 than the colder climates of Central or Northern Europe. To investigate whether distribution of
231 *R. macrosoma* is either natural or the result of human dispersal, several analyses using
232 hierarchical AMOVA were performed (Excoffier et al. 1992) using the Kimura 2P distance
233 method with: 1) all populations in one group; 2) populations per country; and 3) two
234 geographical groups (Eastern *vs* Western populations) considering the areas of greater
235 diversity (Hungary, Romania, Serbia and Crete, Greece) *vs* lower-diversity (Spain, France,
236 Germany, Italy and the Czech Republic), respectively. All population genetic analyses were
237 performed using Arlequin v. 3.5.2.2 software (Excoffier and Lischer 2010) and only sampling
238 sites from which more than three individuals were sequenced for *coxI* were included in the
239 analysis (resulting in a total of 22 sampling points in nine countries). To investigate
240 evolutionary relationships and mutational differences between haplotypes, as well as the
241 geographical distribution of haplotypes, a haplotype network was built based on the transitive
242 consistency score (TCS) network (Clement et al. 2002) implemented in Population Analysis
243 with Reticulate Trees (PopART) v. 1.7 (http:/popart.otago.ac.nz). A rarefraction approach was
244 evaluated using the R package *Spider* v. 1.5.0. (Brown et al. 2012). Isolation by distance (IBD)
245 was assessed with a Mantel test using the *adegenet* package (Jombart 2008) in R based on the
246 *coxI* marker. The Mantel test was performed between genetic distances based on Edwards'
247 distance (Euclidean) and geographical distances (Km) using 10,000 randomizations.
248 Distances between populations points were calculated using the great-circle distance between
249 populations in the *gdistance* package (van Etten 2017) in R. Plots were drawn using the
250 Modern Applied Statistics with S (*MASS*) package (Venables and Ripley 2002) in R.
251
252 **Phylogenetic analyses.** The 28S rRNA and the partial *coxI* sequences were used for
253 phylogenetic analyses. Outgroup taxa for each dataset were chosen following previously
254 published studies (Van Den Berg et al. 2016; Palomares-Rius et al. 2018). Multiple sequence
255 alignments of the different genes were generated using the FFT-NS-2 algorithm of MAFFT
256 v.7.450 (Katoh et al. 2019). Sequence alignments were visualized using BioEdit (Hall 1999)
257 and edited with Gblocks v. 0.91b (Castresana 2000) on the Castresana Laboratory server
258 (http://molevol.cmima.csic.es/castresana/Gblocks_server.html) using options for less

259 stringent selection (minimum number of sequences for a conserved or a flanking position:
260 50% of the number of sequences + 1; maximum number of contiguous nonconserved
261 positions: 8; minimum length of a block: 5; allowed gap positions: with half). Phylogenetic
262 analyses of the sequence datasets were based on Bayesian inference (BI) using MrBayes v.
263 3.1.2 (Ronquist and Huelsenbeck 2003) and maximum likelihood (ML) using PAUP* 4b10
264 (Swofford 2003). The best-fit model of DNA evolution was obtained using JModelTest
265 v.2.1.7 (Darriba et al. 2012) with the Akaike Information Criterion (AIC). The best-fit model,
266 the base frequency, the proportion of invariable sites, and the gamma distribution shape
267 parameters and substitution rates of the AIC were input to MrBayes for the phylogenetic
268 analyses. We used an unlinked general time-reversible model with invariable sites and a
269 gamma-shaped distribution (GTR + I + G) for the D2-D3 expansion segments of 28S rRNA
270 and the partial *coxI*. These BI analyses were run separately for each dataset using four Markov
271 chains for 2×10^6 generations for each molecular marker. The Markov chains were sampled
272 at intervals of 100 generations. Two runs were conducted for each analysis. After discarding
273 burn-in samples of 30% and evaluating convergence, the remaining samples were retained for
274 further analyses. The topologies were used to generate a 50% majority-rule consensus tree.
275 Posterior probabilities (PP) are given for appropriate clades. In the ML analysis, the estimation
276 of the support for each node was obtained through bootstrap analysis with 200 fast-step
277 replicates. Trees from all analyses were visualized using FigTree v.1.4.4
278 (http://tree.bio.ed.ac.uk/software/figtree/) (Page 1996).
279

280 **Species delimitation.** To test whether the sequence datasets represented single or multiple
281 species, the General Mixed Yule Coalescent (GMYC) (Fujisawa and Barraclough 2013; Pons
282 et al. 2006) and Automatic Barcode Gap Discovery (ABGD) (Puillandre et al. 2012) methods
283 were applied. The ABGD analyses were processed using the online server
284 (https://bioinfo.mnhn.fr/abi/public/abgd/) with the default program settings. Distances were
285 calculated utilizing the Jukes-Cantor (JC69) model and the Kimura (K80) model of nucleotide
286 substitution.

287 The GMYC algorithm compares two alternative models: 1) a single coalescence model
288 that assumes a single species, and 2) a model that combines a coalescent model of intraspecific
289 branching with a Yule model of interspecific branching, thus assuming multiple species. The
290 location of the switch (threshold T) from speciation to coalescence nodes is fitted on the tree,
291 resulting in an estimate of species diversity. The ultrametric tree was produced in BEAST v.
292 1.10.4 (Drummond et al. 2018) without outgroups and duplicated haplotypes were excluded

293 from the dataset using FaBox 1.5 (Villesen 2007). For the 28S rRNA dataset, the set priors
294 were as follows: substitution model = GTR; base frequencies = estimated; site heterogeneity
295 model = gamma; length of chain = 5×10^7 generations. For the *coxI* dataset, substitution model
296 = GTR; base frequencies = estimated; site heterogeneity model = invariant site; length of chain
297 = 1×10^7 generations, and different codon positions were regarded as different partitions. For
298 both molecular markers, the uncorrelated lognormal relaxed clock and constant size
299 coalescent prior were used as the clock type and tree model, respectively. Tracer v. 1.7.1
300 (Rambaut et al. 2018) was used to check for effective sample size values (ESS > 200).
301 TreeAnnotator v. 1.10.4 (Drummond et al. 2018) was used to obtain consensus trees, using a
302 burn-in of 10%. The ultrametric tree produced by BEAST was submitted to R using the
303 packages *ape* (Paradis and Schliep 2018) and *splits* (Ezard et al. 2017).
304 We relied on a conservative consensus approach similar to that described in Hauquier
305 et al. (2017) to maximize the reliability of species boundaries using the different species
306 delimitation methods. More specifically, we recognized species clades that: 1) received high
307 nodal support (at least 75% bootstrap support in the ML tree and 90% PP in the BI phylogeny),
308 2) showed compatible patterns based on statistical parsimony, ABGD and GMYC analyses,
309 and 3) formed concordant clades in the trees inferred from nuclear and mitochondrial markers
310 and/or expressed different morphological characteristics.
311
312
313 **RESULTS**
314
315 ***Rotylenchulus macrosoma:* expanded distribution, new host species and soil infestation**
316 **levels.** We identified 28 new locations where *R. macrosoma* occurred, which included several
317 European countries and crop species, in addition to those reported by Palomares-Rius et al.
318 (2018) (Table 1). Thus, *R. macrosoma* is more widely distributed in Europe than previously
319 reported, with first reports of the species in eight European countries (the Czech Republic,
320 France, Germany, Hungary, Italy, Romania, Serbia and Portugal) (Table 1). Except for
321 Portugal, we sampled more than one location in all countries, and in Hungary we sampled a
322 maximum of 7 locations (Table 1). Soil infestation densities ranged from 3 to 1760 individuals
323 per 100 cm^3 soil. Four new host-plant species including corn, pea (*Pisum sativum*), wheat and
324 almond (*Prunus dulcis*)-peach (*P. persica*) hybrid rootstock, were added to the list of known
325 host plants, which include bean, chickpea, hazelnut, peanut, soybean, and wild and cultivated
326 olive (Table 1). Samples exhibiting high population densities and the presence of abundant

327 eggs and mature sedentary females were found. In all the samples, the morphometrics and
328 morphological characteristics agreed well with previous descriptions of *R. macrosoma* from
329 other populations (Fig. 1).
330
331 **Molecular variability and population genetic structure.** The *coxI* fragment was sequenced
332 (336 bp) from 210 individuals, and 16 haplotypes were identified. There were 64 variable sites
333 without any insertions or deletions. In those individuals with different *coxI* haplotypes and
334 those from different populations, the 28S rRNA fragment was sequenced and 13 haplotypes
335 were found among 46 isolates sequenced (Table 1). The alignment and analysis of the
336 mutations in the *coxI* coding region showed that the mutations were located at the 1st and 3rd
337 codon positions (Fig. S1). The mutations at the 1st codon position were distributed in two
338 regions, while those at the 3rd position were distributed throughout the alignment, showing
339 that these sequences were likely true coding regions. Three stop codons (TAGs) were found
340 in haplotypes coi-H1, coi-H4, coi-H9-coi-H12 and coi-H14-coi-H16 at three variable
341 positions (12, 68 and 109 in the amino acid alignment). All of the stop codon positions were
342 coincident with a tyrosine (Y) residue in the sequences from other isolates (Fig. S2). The
343 alignment of the D2-D3 expansion segments of the 28S rRNA sequence showed some
344 heterozygous nucleotide positions, while for the same position other haplotypes showed a
345 clear and unique nucleotide (data not shown).
346 The number of *coxI* and D2-D3 region haplotypes per population ranged from 1 to 3,
347 and from 1 to 2, respectively (Table 1). Using rarefaction, the number of differentiated
348 individuals based on *coxI* haplotypes reached saturation at approximately 150 sequences (Fig.
349 S3). The distribution of haplotypes per country (Fig. 2A and Table 2) showed high diversity
350 in Eastern European countries (Greece, Hungary, Romania, and Serbia), while in Western
351 Europe the diversity was either lower, or only one haplotype was detected, even when many
352 populations were sequenced (as in France). There were three clades of related haplotypes (Fig.
353 2B): 1) Clade I, with haplotypes coi-H1, coi-H2, coi-H8 and coi-H9 detected in Greece, Spain
354 and Portugal; 2) Clade II, with haplotypes coi-H3, coi-H7 and coi-H13 detected in the Czech
355 Republic, France, Germany, Hungary, Italy, Serbia, and Spain); and 3) Clade III, with the
356 remaining haplotypes (coi-H4, coi-H5, coi-H6, coi-H10, coi-H11, coi-H12, coi-H14, coi-H15
357 and coi-H16) located in Hungary, Romania and Serbia. Each group showed different and
358 characteristic patterns depending on the country. For example, Crete (Greece), is an island,
359 and showed specific haplotypes that were not shared with other countries and presented
360 notable molecular differences compared to the other haplotypes from continental Europe.

361 Clade II contained the most prevalent and widespread haplotypes including coi-H3 and coi-
362 H7, while Clade III contained the greatest number of different haplotypes with small
363 differences in nucleotides, which were grouped in a restricted area (central Europe) and were
364 detected in only three countries. In some countries, both prevalent and rare haplotypes were
365 found (as in the Czech Republic, Hungary, Serbia, and Spain). However, within a given
366 nematode population, the co-occurrence of both prevalent haplotypes and rare haplotypes was
367 only found in Bagamer (Hungary) and Reus (northern Spain), while co-occurrence of the most
368 prevalent haplotypes (coi-H3 and coi-H7) together in the same population was found in
369 Bonyhad (Hungary), Bagamer (Hungary), Moretta (Italy) and Ancona (Italy) (Table 1).

370 The analysis to investigate whether sequence evolution followed a neutral model based
371 on all samples as a single population showed significant results (Tajima's D = 2,306, $P < 0.05$;
372 Fu's Fs = 31,052, $P = < 0.0001$). When analyzed individually, only the population from
373 Bonyhad (Hungary) exhibited a significant *P* value for Tajima's D statistic, while none of the
374 populations showed significance for Tajima's D statistic or Fu's Fs test; all values of Fu's Fs
375 test were greater than 0 in the populations where it was possible to calculate the statistic (Table
376 S1). Based on all samples as a single population, Tajima's D statistic and Fu's Fs test rejected
377 the null hypothesis of demographic stability. Pairwise F_{st} values for each country using the
378 Kimura 2P distance method (Table 3), and those obtained for the populations (Table S2) show
379 that for both the country and population levels there was population genetic structure, with
380 the majority of values ranging from large (0.15 to 0.25) to very large (>0.25), following
381 Wright's division (Wright 1978). Most of the comparisons were significant. Only 5 pairwise
382 F_{st} comparisons were not significant (Spain *vs*. France, France *vs*. Italy, France *vs*. Serbia,
383 Czech Republic *vs*. Germany and Hungary *vs*. Serbia). We also detected genetic structure
384 among populations of *R. macrosoma* based on hierarchical AMOVA for the *coxI* marker when
385 based on the 23 populations (n $\geqslant$ 3 reports) or the 9 source countries (Table 4). When all
386 populations were considered, most of the molecular variation was found among populations
387 (97.5%), while the variation within the populations was minimal (2.53%). Based on countries,
388 the majority of the genetic variation was found among countries (69.71%), followed by that
389 among populations within countries (27.95%). The variance groupings were significant in all
390 cases. Separation of the populations into two large geographical groups (Western *vs* Eastern
391 in Europe) showed that most variation was found among populations (72.49%), although some
392 variation between the two groups was also detectable (25.31%).

393 The analysis of population isolation by distance (IBD) using the *coxI* marker showed
394 a weak correlation ($r = 0.3579$, $P = 0.0027$) (Fig. S4A). There was one grouping of data points

identified, and several minor groupings, based on the analysis (Fig. S4B). The minor groupings could be associated with the distribution of correlated points in the figures, in which three major lines of genetic distances were observed, which were related mostly to more distant and differentiated populations (i.e., Cretan and Greek populations) and the presence of *R. macrosoma* in central Europe that exhibited genetic differences (Fig. S4C).

Phylogeny and species delimitation. The *coxI* phylogeny (Fig. 3) showed a basal position for haplotypes coi-H1 and coi-H8 (both unique to Crete and Greece). The main continental European haplotypes formed a well-supported clade within which haplotypes coi-H2 and coi-H9 (from Spain and Portugal) occupied a basal position. These haplotypes were unique to the Iberian Peninsula (Fig. 2). Other prevalent haplotypes including coi-H3 and coi-H7 formed a well-supported clade, that also housed coi-H13, a haplotype unique to Spain. The remaining haplotypes which came from Serbia, Romania and Hungary (central Europe), formed a separate clade (Clade III). In contrast, the D2-D3 expansion segments of the 28S rRNA phylogeny formed loose clades, with the exception of the basal clade from Crete (Greece). Several D2-D3 haplotypes had more than one haplotype that corresponded to the *coxI* sequences, as was the case for 28S-H5, 28S-H9 and 28S-H8. There was a congruent phylogenetic relationship of clades between the *coxI* and D2-D3 expansion segments of 28S rRNA haplotypes, as was seen between the unique Greek and Iberian Peninsula haplotypes. The D2-D3 expansion segments of 28S rRNA showed only a few nucleotides differences providing information for the inference of phylogenies, and only haplotypes with important differences resulted in congruence between the two phylogenies.

The species delimitation study showed congruence for some clades according to both markers (the *coxI* and the D2-D3 expansion segments of 28S rRNA genes) with good congruence between clades of haplotypes in the Crete populations (coi-H1 and coi-H8 haplotypes and 28S-H1 and 28S-H2 haplotypes), whereas weaker PP support and separation of the two haplotypes was observed with the ML analysis (Fig. 5). However, the clade of coi-H1 and coi-H8 was well-supported in the ultrametric phylogenetic tree generated with additional species of the genus *Rotylenchulus* according to the two species separation methods (Fig. S5 and S6). The applied species delimitation methods (GMYC and ABGD) separated the Cretan haplotypes as a group (Fig. S5 and S6), with the exception of the GMYC single method and ABGD method using a 5 species model for the 28S rRNA marker data.

The morphological differences in these populations were discussed previously (Palomares-Rius et al. 2018). Only minor morphometric differences were found in the~~se~~

429 populations compared to the original description. Those previously reported in the
430 Mediterranean Basin had the following measurements: body length (Cretan population, 428-
431 526 *vs* original population, 520-640, Spanish population, 432-520 µm), stylet (15-21 *vs*
432 original population, 18-22, Spanish population, 16-20 µm), a (body length/maximum body
433 width) ratio (Cretan population, 26.1-31.6 *vs* original population, 30-38, Spanish population,
434 27.6-32.1), c' (tail length/body width at anus) ratio (Cretan population, 2.6-4.0 *vs* original
435 population, 3.7-5.0, Spanish population, 2.6-4.0), V ((distance from anterior end to
436 vulva/body length) × 100) ratio (Cretan population, 58-65 *vs* original population, 63-68,
437 Spanish population, 59-66), and o ((distance from stylet base to dorsal pharyngeal
438 opening/body length) × 100) ratio (Cretan population, 105-156 *vs* original population, 139-
439 188, Spanish population, 116-156) (Palomares-Rius et al. 2018). The morphometric results
440 did not support the separation of the Cretan haplotypes as a distinct species.
441
442
443 **DISCUSSION**
444
445 *Rotylenchulus macrosoma* had previously been reported from six Mediterranean
446 countries (Dasgupta et al. 1968; Castillo et al. 2003; Van den Berg et al. 2016; Palomares-
447 Rius et al. 2018; Sikora et al. 2018; Qing et al. 2019), establishing a Mediterranean-centric
448 distribution. However, the new geographic locations in which *R. macrosoma* has been
449 identified brings into question the former categorization of this nematode as a strictly
450 Mediterranean species. The presence of *R. macrosoma* in localities in Northern Europe (with
451 colder winters and moister soil conditions) suggests flexibility in its ecological requirements
452 and survival strategies. As described in the Introduction, *R. reniformis* has high survival
453 potential by exploiting several strategies (the existence of an anhydrobiotic form, egg survival,
454 etc.), which may be shared by *R. macrosoma*. The soil densities found at some sample
455 locations may indicate potential damage to plants. However, impact is difficult to gauge, as
456 the hosts were not assessed for damage, and some samples came from farmers with very
457 limited host species information. In pot-based tests, *R. reniformis* in cotton had a damage
458 threshold of 16 individuals per 200 cm^3 of soil (Sud et al. 1984). Other data suggest significant
459 increases in cotton yield after nematicide application when pretreatment nematode densities
460 were in the range of 100-250 nematodes per 100 cm^3 of soil (Davis et al. 2018). No data
461 regarding the damage threshold for *R. reniformis* or *R. macrosoma* in corn or wheat are
462 available. In our data, 13 sampling locations had nematode densities >100 nematodes per 100

463 cm^3 soil. Our samples were collected mostly in the middle of the cropping season, and do not
464 provide information on nematode populations at other possibly critical points during crop
465 growth.

466 We identified new hosts for *R. macrosoma* including corn, pea, wheat and an almond-
467 peach hybrid rootstock, in addition to those hosts already characterized (olive, peanut, bean,
468 banana (*Musa* × *paradisiaca*) and hazelnut) (Dasgupta et al. 1968; van den Berg et al. 2012;
469 Castillo et al. 2003; Palomares-Rius et al. 2018). Cotton, pepper (*Capsicum annuum*), winter
470 wheat and sour orange (*Citrus aurantinum*) were reported not to be hosts of *R. macrosoma*
471 (Cohn and Mordechai 1988; Robinson et al. 1997). However, we found winter wheat to be a
472 host at three of the 37 wheat sample locations. Potential explanations for the contrary
473 observation regarding wheat as a host include lack of research to confirm whether *R.*
474 *macrosoma* parasitizes wheat, and the fact that most phytonematological studies on wheat
475 have been focused on cyst and root-lesion nematodes, rather than on reniform nematodes
476 (Nicol et al. 2003; Smiley et al. 2005). Other possible explanations include the low *R.*
477 *macrosoma* population density in soil, the lack of apparent impact on wheat yield and the
478 difficulties in accurate species identification in general nematode surveys, as *R. macrosoma*
479 is easily confused with *Helicotylenchus* spp.
480

481 **Molecular diversity and population genetic structure of *Rotylenchulus macrosoma*.** The
482 sequencing of more individuals from populations studied by Palomares-Rius et al. (2018) and
483 additional populations from other European countries showed the presence of a stop codon
484 (TAG) in some haplotypes of *R. macrosoma* using the alternative flatworm mitochondrial
485 genetic code (coi-H1, coi-H4, coi-H9, coi-H10, coi-H11, coi-H12, coi-H14, coi-H15, coi-
486 H16) (Fig. S2). The stop codon has not been observed in other species of this genus including
487 *R. reniformis, R. macrosomoides* and *R. macrodoratus.* Although only a limited number of
488 individuals have been sequenced, these species show correct translation using the alternative
489 flatworm code (Palomares-Rius et al. 2018; van den Berg et al. 2016). We believe that the
490 stop codon (TAG) encodes a tyrosine (Y) because the residue has been found at this alignment
491 position in other haplotypes of *R. macrosoma*, and in other species of the genus, and even in
492 phylogenetically related nematode species including *Globodera pallida* and *Rotylenchus*
493 *magnus* based on Blastn searches in NCBI. The mutations occurred at the first and third codon
494 positions, which showed that the gene could be functional within the mitochondrial genome,
495 even with the stop codon present in some haplotypes. We used the same primer set for other
496 populations of this species and other species of the genus (Palomares-Rius et al. 2018). Clear

497 peaks in our chromatograms from Sanger sequencing indicate that our sequences were true
498 and the coding sequence beyond the stop codon position reinforces the idea that these
499 haplotypes (coi-H3, coi-H9-H12 and coi-H14-H16) have proper coding sequences. However,
500 without mitochondrial sequences of all the haplotypes from different species, and considering
501 the short fragment of the gene sequenced, it is not possible to corroborate these observations
502 and demonstrate that the sequence with the stop codon is not a pseudogene. Jacob et al. (2009)
503 also found an exception to the translation code of Nematoda in *Radopholus similis* and *R.*
504 *arabocoffeae*, where the codon (TAA) also encodes the amino acid tyrosine (Y).

505 The results of the different genetic analyses of the mtDNA data supported the existence
506 of pronounced genetic structure among populations of *R. macrosoma* found in Europe, with a
507 large number of haplotypes of the *coxI* gene and the D2-D3 expansion segments of the 28S
508 rRNA gene. Both Tajima´s D and Fu´s Fs statistics rejected the null hypothesis of selective
509 neutrality and demographic stability when all the data were combined. However, when the
510 populations were analyzed individually, the null hypothesis of selective neutrality and
511 demographic stability could not be rejected. In this case, the number of haplotypes per
512 population was low, which could be due to either random introduction events or selection for
513 particular genotypes, which may be observed when resistant cultivars or other management
514 strategies are applied, including application of sublethal concentrations of nematicides
515 (Young and Hartwig 1988; Meher et al. 2009). The positive values of Tajima's D and Fu's Fs
516 could suggest that the *R. macrosoma* population may have suffered a recent bottleneck event
517 (Tajima 1989; Fu 1997). In this study, two dominant haplotypes were defined in the *coxI*
518 dataset (coi-H1 and coi-H3). The expansion in distribution among fields and regions of some
519 soil organisms including PPNs could be related to transfer of infested plant material or soil
520 adhered to machinery. Therefore, the survival of possibly a few nematodes for every field
521 introduction could create a bottleneck effect, and it may explain some of our results (only one
522 haplotype per field in the majority of the fields), or just the existence of geographically
523 restricted haplotypes in some areas (i. e. coi-H11). In addition to the two prevalent haplotypes
524 in Europe (coi-H3 and coi-H7), there were other haplotypes identified that are restricted to
525 specific areas in Europe (clade I and clade II haplotypes, Fig. 2B). While we detected some
526 areas in Central Europe with a large number of different haplotypes, there was low variability
527 among them (clade III, Fig. 2B).

528 There was evidence of pronounced genetic structure at different scales of the
529 populations of *R. macrosoma* sampled. The AMOVA based on countries showed that although
530 the majority of the variation was accounted for among countries (69.47%), a proportion of

variation was found among populations within countries (27.95%), but relatively little variation (2.34%) within populations. However, AMOVA based on the separation between Western countries (fewer haplotypes with 70 sequenced nematodes, 8 populations) vs. Eastern countries (more haplotypes with 126 sequenced nematodes, 15 populations) found that although some variation was explained between Eastern and Western European groups (25.31%), most variation was found among populations within the two groups (72.49%). This could be a result of dominant haplotypes (coi-H3 and coi-H7) being shared between artificial groups (political divisions based on countries). The IBD test showed a correlation with geographical distance, but the maximum genetic distances were not correlated with the maximum genetic separation between populations. The genetic differences and the patchy distribution of *R. macrosoma*, including the large number of fields with positive samples in Central Europe, may have influenced the result. The IBD could be influenced by habitat configuration and the maximum migration distance (van Strien et al. 2015). In our case, considering the limited dispersal of soil PPNs, dispersion by human activities is likely to play a greater role in altering the natural dispersal pattern of the species.

The phylogenetic analysis of the *coxI* and D2-D3 expansion segments of 28S rRNA markers showed that some haplotypes were closely related to the ancestral haplotype for *R. macrosoma* (Fig. 3). coi-H1 and coi-H8 haplotypes from Crete (Greece) were closely related to the outgroups for both phylogenetic trees and coi-H2 and coi-H9 were unique to the Iberian Peninsula and closely related to Cretan haplotypes in the TCS haplotype network (Fig. 2B), while other haplotypes occupied an intermediate position, including coi-H3, coi-H13 and coi-H7. This result indicated a restricted distribution for some haplotypes. However, our data from natural environments are limited; only one sample was obtained from wild olive in southern Spain (Vejer). We hypothesize that human activities including agricultural management and trade could be important factors in the expansion and movement of *R. macrosoma* among populations across Europe through bi-directional dispersal, as described for other pathogens (McDonald and Stukenbrock 2016). Areas where *R. macrosoma* has been previously observed, such as continental Greece, should be investigated in future studies. Other locations could harbor different haplotypes and may present different scenarios regarding phylogeographic hypotheses. Additionally, the current distribution of *R. macrosoma* could expand to new areas in Europe due to the effect of global climate change.

Species delimitation. The methods and stringent criteria used to detect more than one species in the dataset showed that the Cretan populations were genetically separate from the other

565 populations, but did not meet all of our criteria outlined in the Material and Methods section,
566 and so could not be considered a separate species. The species delimitation analyses did not
567 support the separation of the Cretan populations as a distinct species based on data from both
568 markers that we used. Additionally, the Cretan populations showed only a few morphological
569 differences in comparison with the continental populations of *R. macrosoma*.
570
571 **Conclusions and Perspectives.** This study described a wider distribution of *R. macrosoma* in
572 Europe compared to what was previously assumed, and in some cases the population densities
573 were close to pathogenic levels. The species had pronounced genetic structure, and some
574 haplotypes were specific to countries (Greece) or geographical areas (Iberian Peninsula).
575 Wider geographic sampling is required to define the limits of the species distribution
576 (including the Middle East), which may result in new haplotypes, and will provide a more a
577 complete picture of the distribution and host range of *R. macrosoma*.
578
579
580 **ACKNOWLEDGEMENTS**
581
582 The authors thank G. León Ropero and J. Martín Barbarroja (IAS-CSIC) for their
583 excellent technical assistance. The authors acknowledge the Spanish Ministry of Science,
584 Innovation and Universities for the financial support of this article under the project
585 "RTI2018-095925-A-I00". The first author acknowledges the Spanish Ministry of Economy
586 and Competitiveness for the "Ramon y Cajal" Fellowship RYC-2017-22228. A. Archidona-
587 Yuste is a recipient of the Humboldt Research Fellowship for Postdoctoral Researchers at
588 Helmholtz Centre for Environmental Research-UFZ, Leipzig, Germany. R. Cai acknowledges
589 the China Scholarship Council (CSC) for financial support.
590
591
592 **LITERATURE CITED**
593
594 Arias, R. S., Stetina, S. R., Tonos, J. L., Scheffler, J. A. and Scheffler, B. E. 2009.
595 Microsatellites reveal genetic diversity in *Rotylenchulus reniformis* populations. J.
596 Nematol. 41:146-156.
597 Artero, J., Bello, A., and Gómez-Barcina, A. 1977. *Rotylenchulus reniformis* Linford et
598 Oliveira, 1940 (Nematoda: Rotylenchulinae) en España. Nematol. Medit. 5:247-252.

599 Bowles, J., Blair, D., and McManus, D. P. 1992. Genetic variants within the genus
600 *Echinococcus* identified by mitochondrial DNA sequencing. Mol. Biochem. Parasitol.
601 54:165-174.
602 Brown, S. D. J., Collins, R. A., Boyer, S., Lefort, M. C., Malumbres-Olarte, J., Vink, C. J.,
603 and Cruickshank, R. H. 2012. Spider: An R package for the analysis of species identity
604 and evolution, with particular reference to DNA barcoding. Mol. Ecol. Resour. 12:562-
605 565.
606 Castillo, P., and Gómez-Barcina, A. 1993. Plant-parasitic nematodes associated with tropical
607 and subtropical crops in southern Spain. Nematol. Medit. 5:45-47.
608 Castillo, P., Vovlas, N., and Troccoli, A. 2003. The reniform nematode, *Rotylenchulus*
609 *macrosoma*, infecting olive in Southern Spain. Nematology 5:23-29.
610 Castresana, J. 2000. Selection of conserved blocks from multiple alignments for their use in
611 phylogenetic analysis. Mol. Biol. Evol. 17:540-552.
612 Clement, M., Snell, Q., Walker, P., Posada, D., and Crandall, K. 2002. TCS: Estimating gene
613 genealogies. Parallel and Distributed Processing Symposium, International Proceedings
614 2:184.
615 Cohn, E., and Mordechai, M. 1988. Morphology and parasitism of the mature female of
616 *Rotylenchulus macrosomus*. Rev. Nématol. 11:385-389.
617 Coolen, W. A. 1979. Methods for extraction of *Meloidogyne* spp. and other nematodes from
618 roots and soil. In: Root-knot nematodes (*Meloidogyne* species). Systematics, biology and
619 control. Lamberti F., Taylor C.E. (Editors), Academic Press, New York, USA, pp. 317-
620 329.
621 Darriba, D., Taboada, G. L., Doallo, R., and Posada, D. 2012. jModelTest 2: more models,
622 new heuristics and parallel computing. Nat. methods 9:772.
623 Dasgupta, D. R., Raski, D. J., and Sher, S. A. 1968. A revision of the genus *Rotylenchulus*
624 Linford and Oliveira, 1940 (Nematoda: Tylenchidae). Proc. Helminthol. Soc. Wash.
625 35:169-192.
626 Davis, F. D., Galbieri, R. and Asmus, G. L. 2018. Nematode parasites of cotton and other
627 tropical fiber crops. In: Plant parasitic nematodes in subtropical and tropical agriculture.
628 (R. A. Sikora, D. Coyne, J. Hallmann and P. Timper. Eds.) pp. 738-754. Wallingford,
629 UK. CAB International.
630 De Ley, P., Félix, M. A., Frisse, L. M., Nadler, S. A., Sternberg, P. W., and Thomas, K. W.
631 1999. Molecular and morphological characterisation of two reproductively isolated
632 species with mirror-image anatomy (Nematoda: Cephalobidae). Nematology 1:591-612.

633 Derycke, S., Remerie, T., Backeljau, T., Vierstraete, A., Vanfelteren, J., Vincx, M., and
634 Moens, T. 2008. Phylogeography of the *Rhabditis* (*Pellioditis*) marina species complex:
635 evidence for long-distance dispersal, and for range expansions and restricted gene flow
636 in the northeast Atlantic. Mol. Ecol. 17:3306-3322.
637 Excoffier, L., and Lischer, H. E. 2010. Arlequin suite ver 3.5: a new series of programs to
638 perform population genetics analyses under Linux and Windows. Mol. Ecol.
639 Resour.10:564-567.
640 Excoffier, L., Smouse, P. L., and Quattro, J. M. 1992. Analysis of molecular variance inferred
641 from metric distances among DNA haplotypes: Application to human mitochondrial
642 data. Genetics 131:479-491.
643 Ezard T., Fujisawa T., and Barraclough T. 2017. splits: SPecies' LImits by Threshold
644 Statistics. R package version 1.0-19/r52.https://R-Forge.R project.org/projects/splits/
645 Fu, Y. X. 1997. Statistical tests of neutrality of mutations against population growth,
646 hitchhiking and background selection. Genetics 147:915-925.
647 Fujisawa, T., and Barraclough, T. G. 2013. Delimiting species using single-locus data and the
648 Generalized Mixed Yule Coalescent (GMYC) approach: A revised method and
649 evaluation on simulated datasets. Syst. Biol. 62:707-724.
650 Ganji, S., Sanders, W. S., Stokes, J. V., Showmaker, K., Bartlett, B., Wang, H., Wubben, M.,
651 McCarthy, F., Magbanua, Z., and Peterson, D. 2013. The genome of reniform nematode,
652 *Rotylenchulus reniformis*. In: Proceedings of the 10th Conference of the Mid-South
653 Computational Biology and Bioinformatics Society, April 5-6, 2013, Columbia, MO,
654 USA.
655 Gaur, H. S., and Perry, R. N. 1991. The biology and control of the plant parasitic nematode,
656 *Rotylenchulus reniformis*. Agric. Zool. Rev. 4:177-212.
657 Gomez, A., and Lunt, D. 2006. Refugia within refugia: patterns of phylogeographic
658 concordance in the Iberian Peninsula, pp. 155–188 in Phylogeography of Southern
659 European Refugia, edited by S. Weiss and N. Ferrand. Springer, Dordrecht, The
660 Netherlands.
661 Gutiérrez-Gutiérrez, C., Castillo, P., Cantalapiedra-Navarrete, C., Landa, B. B., Derycke, S.,
662 and Palomares-Rius, J. E. 2011. Genetic structure of *Xiphinema pachtaicum* and *X. index*
663 populations based on mitochondrial DNA variation. Phytopathology 101:1168-1175.
664 Hall, T. A. 1999. BioEdit: a user-friendly biological sequence alignment editor and analysis
665 program for windows 95/98/NT. Nucleic Acids Symp. Ser. 41:95-98.

666 Hauquier, F., Leliaert, F., Rigaux, A., Derycke, S., and Vanreusel, A. 2017. Distinct genetic
667 differentiation and species diversification within two marine nematodes with different
668 habitat preference in Antarctic sediments. BMC Evol. Biol. 17:120. DOI
669 10.1186/s12862-017-0968-1
670 Hewitt, G. M., 2001 Speciation, hybrid zones and phylogeography—or seeing genes in space
671 and time. Mol. Ecol. 10:537-549.
672 IPCC. 2019. Intergovernmental Panel on Climate Change. https://archive.ipcc.ch/index.htm
673 Jacob, J. E. M., Vanholme, B., Van Leeuwen, T., and Gheysen, G. 2009. A unique genetic
674 code change in the mitochondrial genome of the parasitic nematode *Radopholus similis*.
675 BMC Res. Notes 2:192. doi:10.1186/1756-0500-2-192.
676 Jombart, T. 2008. Adegenet: a R package for the multivariate analysis of genetic markers.
677 Bioinformatics 24:1403-1405.
678 Katoh, K., Rozewicki, J., and Yamada, K. D. 2019. MAFFT online service: multiple sequence
679 alignment, interactive sequence choice and visualization. Brief. Bioinform. 20:1160-
680 1166.
681 Leach, M., Agudelo, P. and Lawton-Rauh, A. 2012. Genetic variability of *Rotylenchulus*
682 *reniformis*. Plant Dis. 96:30-36.
683 McDonald, B. A. and Stukenbrock, E. H. 2016. Rapid emergence of pathogens in agro-
684 ecosystems: global threats to agricultural sustainability and food security. Philos Trans
685 R Soc Lond B Biol Sci. 20160026. doi: 10.1098/rstb.2016.0026.
686 Meher, H. C., Gajbhiye, V. T., Chawla, G., and Singh, G. 2009. Virulence development and
687 genetic polymorphism in *Meloidogyne incognita* (Kofoid & White) Chitwood after
688 prolonged exposure to sublethal concentrations of nematicides and continuous growing
689 of resistant tomato cultivar. 2009. Pest Manag Sci 65, 1201-1207
690 Nei, M. 1987. Molecular evolutionary genetics. New York: Columbia university press.
691 Nicol, J., Rivoal, R., Taylor, S., and Zaharieva, M. 2003. Global importance of cyst
692 (*Heterodera* spp.) and lesion nematodes (*Pratylenchus* spp.) on cereals: Yield loss,
693 population dynamics, use of host resistance, and integration of molecular tools.
694 Nematology Monographs and Perspectives 2:1-19.
695 Nyaku, S. T., Sripathi, V. R., Kantety, R. V., Cseke, S. B., Buyyarapu, R., Mc Ewan, R., Gu,
696 Y. Q., Lawrence, K., Senwo, Z., Sripathi, P., George, P. and Sharma, G. C. 2014.
697 Characterization of the reniform nematode genome by shotgun sequencing. Genome
698 57:209-221.

699 Page, R. D. 1996. TreeView: an application to display phylogenetic trees on personal
700 computers. CABIOS. 12:357-358.
701 Palomares-Rius, J. E., Cantalapiedra-Navarrete, C., Archidona-Yuste, A., Tzortzakakis, E. A.,
702 Birmpilis, I. G., Vovlas, N., Subbotin, S. A., and Castillo, P. 2018. Prevalence and
703 molecular diversity of reniform nematodes of the genus *Rotylenchulus* (Nematoda:
704 Rotylenchulinae) in the Mediterranean Basin. Eur. J. Plant Pathol. 150:439-455.
705 Palomares-Rius, J. E., Escobar, C., Cabrera, J., Vovlas, A., and Castillo, P. 2017. Anatomical
706 alterations in plant tissues induced by plant-parasitic nematodes. Front. Plant Sci.
707 8:1987.
708 Paradis E., and Schliep K. 2018. ape 5.0: an environment for modern phylogenetics and
709 evolutionary analyses in R. Bioinformatics 35:526-528.
710 Pons, J., Barraclough, T. G., Gomez-Zurita, J., Cardoso, A., Duran, P. D., Hazell, S., Kamoun,
711 S., Sumlin, W. D., and Vogler, A. P. 2006. Sequence-based species delimitation for the
712 DNA taxonomy of undescribed insects. Syst. Biol. 55:595-609.
713 Puillandre, N., Lambert, A., Brouillet, S., and Achaz, G. 2012. ABGD, Automatic Barcode
714 Gap Discovery for primary species delimitation. Mol. Ecol. 21:1864-1877.
715 Qing, X., Bik, H., Yergaliyev, T. M., Gu, J., Fonderie, P., Brown-Miyara, S., Szitenberg, A.,
716 and Bert, W. 2019. Widespread prevalence but contrasting patterns of intragenomic
717 rRNA polymorphisms in nematodes: Implications for phylogeny, species delimitation
718 and life history inference. Mol. Ecol. Resour. 20:318-332.
719 R Core Team 2019. R: A language and environment for statistical computing. R Foundation
720 for Statistical Computing, Vienna, Austria. http://www.R-project.org/.
721 Rambaut, A., Drummond, A. J., Xie, W., Baele, G., and Suchard, M. A. 2018. Tracer v1.7.1
722 Available online: http://tree.bio.ed.ac.uk/software/tracer.
723 Robinson, A. F. 2007. Reniform in U.S. cotton: when, where, why, and some remedies. Annu.
724 Rev. Phytopathol. 45:263-288.
725 Robinson, A. F., Inserra, R. N., Caswell-Chen, E. P., Vovlas, N., and Troccoli, A. 1997.
726 *Rotylenchulus* species: Identification distribution, host ranges, and crop plant resistance.
727 Nematropica 27:127-180.
728 Rogers, A.R., and Harpending, H. 1992. Population growth makes waves in the distribution
729 of pairwise genetic differences. Mol. Biol. Evol. 9:552-569.
730 Ronquist, F., and Huelsenbeck, J. P. 2003. MRBAYES 3: Bayesian phylogenetic inference
731 under mixed models. Bioinformatics 19:1572-1574.

732 Rozas, J., Ferrer-Mata, A., Sánchez-DelBarrio, J. C., Guirao-Rico, S., Librado, P., Ramos-
733 Onsins, S. E., and Sánchez-Gracia, A. 2017. DnaSP 6: DNA Sequence Polymorphism
734 Analysis of Large Datasets. Mol. Biol. Evol. 34:3299-3302.
735 Showmaker, K. C., Sanders, W. S., Eves-van den Akker, S., Martin, B. E., Platt, R. N.,
736 Stokes, J. V., Hsu, C.Y., Bartlett, B. D., Peterson, D. G., and Wubben, M. J. 2019. A
737 genomic resource for the sedentary semi-endoparasitic reniform nematode,
738 *Rotylenchulus reniformis* Linford & Oliveira. J. Nematol. 51, 1-2. doi:
739 10.21307/jofnem-2019-013
740 Sikora, R. A., Claudius-Cole, B., and Sikora, E. J. 2018. Nematode parasites of food legumes.
741 Pp. 290-345 in (R. A. Sikora, D. Coyne, J. Hallmann and P. Timper. Eds.). Plant Parasitic
742 Nematodes in Subtropical and Tropical Agriculture. Wallingford, UK. CAB
743 International.
744 Smiley, R. W., Whittaker, R. G., Gourlie, J. A., Easley, S. A., and Ingham, R. E. 2005. Plant-
745 parasitic nematodes associated with reduced wheat yield in Oregon: *Heterodera avenae*.
746 J. Nematol. 37:297-307.
747 Subbotin, S. A., Toumi, F., Elekçioglu, I. H., Waeyenberge, L., and Maafi, Z. T. 2018. DNA
748 barcoding, phylogeny and phylogeography of the cyst nematode species of the Avenae
749 group from the genus *Heterodera* (Tylenchida: Heteroderidae). Nematology 20:671-
750 702.
751 Subbotin, S., Waeyenberge, A. L., and Moens, M. 2000. Identification of cyst forming
752 nematodes of the genus *Heterodera* (Nematoda: Heteroderidae) based on the ribosomal
753 DNA-RFLPs. Nematology 2:153–164.
754 Sud, U. C., Varaprasad, K. J., Seshadri, A. R., and Kher, K. K. 1984. Relationship between
755 initial densities of *Rotylenchulus reniformis* and damage to cotton with fit to Seinhorst
756 curves. Ind. J. Nematol. 14:148-151.
757 Swofford, D. L. 2003. PAUP*: Phylogenetic analysis using parsimony (*and other methods),
758 1 version 4.0b 10. Sinauer Associates, Sunderland, Massachusetts.
759 Tajima, F. 1989. Statistical method for testing the neutral mutation hypothesis by DNA
760 polymorphism. Genetics 123:585-595.
761 Van Den Berg, E., and Quénéhervé, P. 2012. Hoplolaimidae. Pages 251-297. In: Practical
762 Plant Nematology (eds. Rosa H. Manzanilla-López and Nahúm Marbán-Mendoza).
763 Biblioteca Básica de Agricultura, Colegio de Postgraduados. Editorial Colegio de
764 Postgraduados. U. Autónoma de Chapingo, México.

765 Van Den Berg, E., Palomares-Rius, J. E., Vovlas, N., Tiedt, L. R., Castillo, P., and Subbotin,
766 S. A. 2016. Morphological and molecular characterisation of one new and several known
767 species of the reniform nematode, *Rotylenchulus* Linford & Oliveira, 1940
768 (Hoplolaimidae: Rotylenchulinae), and a phylogeny of the genus. Nematology 18:67-
769 107.
770 van Etten, J. 2017. R Package gdistance: Distances and routes on geographical grids. Journal
771 of Statistical Software, 76, issue 13, not pages. Doi: 10.18637/jss.v076.i13
772 van Strien, M.J., Holderegger, R., and van Heck, H. J. 2015. Isolation-by-distance in
773 landscapes: considerations for landscape genetics. Heredity 114:27-37.
774 Villesen, P 2007. FaBox: an online toolbox for fasta sequences, Molecular Ecology Notes 7:
775 965-968. doi:10.1111/j.1471-8286.2007.01821.x
776 Xu, X., Qing, X., Xie, J. L., Yang, F., Peng, Y. L., and Ji, H. L. 2020. Population structure
777 and species delimitation of rice white tip nematode, *Aphelenchoides besseyi* (Nematoda:
778 Aphelenchoididae), in China. Plant Pathol. 69:159-167.
779 Young, L. D., and Hartwig, E. E. 1988. Selection pressure on soybean cyst nematode from
780 soybean cropping sequences. Crop Sci. 28:845-847.
781

Figure legends

Fig. 1. Light micrographs of *Rotylenchulus macrosoma* females parasitizing corn roots. A and B) Swollen females parasitizing roots; C) Swollen and non-swollen females; D) Non-swollen female; E) Male.

Fig.2. Haplotype analysis of *coxI* from *Rotylenchulus macrosoma*. A) Distribution map of the haplotypes in the populations sampled in Europe; B) Transitive consistency score (TCS) network analysis with geographic data.

Fig. 3. Comparison of different haplotype phylogenies based on Bayesian inference and maximum likelihood analysis of *Rotylenchulus macrosoma* haplotypes using the *coxI* and D2-D3 regions of 28S rRNA genes. Lines show related populations with their respective haplotypes.

Supplementary figure legends

Fig. S1. Distribution of Single Nucleotide Polymorphisms (SNPs) in the *coxI* region studied in *Rotylenchulus macrosoma*.

Fig. S2. Alignment of amino acid sequences from *coxI* haplotypes in *Rotylenchulus macrosoma*. coxI haplotype accessions: MT075822 (coi-H1); MT075823 (coi-H2); MT075824 (coi-H3); MT075825 (coi-H4); MT075826 (coi-H5); MT075827 (coi-H6); MT075828 (coi-H7); MT075829 (coi-H8); MT075830 (coi-H9); MT075831 (coi-H10); MT075832 (coi-H11); MT075833 (coi-H12); MT075834 (coi-H13); MT075835 (coi-H14); MT075836 (coi-H15); MT075837 (coi-H16). Isolates and specific codes are listed in Table 1

Fig. S3. Rarefaction analysis of *coxI* haplotypes of *Rotylenchulus macrosoma*.

817 **Fig. S4**. Isolation by physical distance and genetic distance of the *coxI* gene between
818 populations of *Rotylenchulus macrosoma* in Europe using the *adegenet* package in R. A)
819 Scatter plot showing the correlation between genetic distance as Edwards' distance
820 (Euclidean) *vs* geographical distances (Km) using great-circle distances; B) Density plot using
821 the library MASS for the correlation between genetic distance as Edwards' distance
822 (Euclidean) *vs* geographical distances (Km) using great-circle distances; C) Isolation by
823 distance is tested using a Mantel test between a matrix of genetic distances and a matrix of
824 geographic distances. The original value of the correlation between the distance matrices is
825 represented by the dot, while histograms represent permuted values (i.e., under the absence of
826 spatial structure). Significant spatial structure is inferred when the original value for the
827 association is out of the reference, permuted distribution.
828
829 **Fig. S5.** Molecular species-delimitation analysis of *Rotylenchulus macrosoma* using *coxI* gene
830 sequence. Two methods were used: a generalized mixed Yule coalescent model (GMYC) and
831 an automatic barcode gap discovery (ABGD) model. Delimitation results are visualized as
832 bars in an ultrametric Bayesian maximum clade credibility tree of the *coxI* gene. For the
833 ABGD analysis, the columns correspond to the 6 and 8 species groupings recovered for
834 different prior intraspecific divergence assumptions. Bayesian posterior probabilities are
835 indicated on the branches. GMYC was studied using single and multiple types of analyses.
836
837 **Fig. S6**. Molecular species-delimitation analysis of *Rotylenchulus macrosoma* using sequence
838 of the D2-D3 expansion segments of 28S rRNA gene. Two methods were used: a generalized
839 mixed Yule coalescent model (GMYC) an automatic barcode gap discovery (ABGD) model.
840 Delimitation results are visualized as bars in an ultrametric Bayesian maximum clade
841 credibility tree of the D2-D3 expansion segments of 28S rRNA gene. For the ABGD analysis,
842 the columns correspond to the 6 and 8 species groupings recovered for different prior
843 intraspecific divergence assumptions. Bayesian posterior probabilities are indicated on the
844 branches. GMYC was studied with single and multiple types of analyses.
845
846
847
848

TABLE 1. Populations of *Rotylenchulus macrosoma* sampled in Europe, indicating host plants, localities and population densities, and the genes sequenced with haplotype identity.

Reference					Haplotype	
Populations number	**Sample code**	**Host-plant**	**Host-plant, locality, province**	***R. macrosoma* individuals/ 100 cm³ soil**	**coxI[a]**	**D2D3[b]**
1	186105	corn	Njegosevo, Vojvodina, Serbia	231	coi-H3 (9)	28S-H5 (1)
2	186111	corn	Bečej, Vojvodina, Serbia	483	coi-H4 (1)	28S-H6 (1)
3	186107	corn	Novi Bečej, Vojvodina, Serbia	18	coi-H14 (5)	28S-H6 (1)
					coi-H15 (3)	28S-H12 (2)
						28S-H13 (2)
4	186231	corn	Nadlac, Arad, Romania	21	coi-H5 (3)	28S-H6 (1)
					coi-H6 (2)	28S-H10 (2)
5	186365	corn	Mircea Voda, Romania	91	coi-H11 (10)	28S-H6 (1)
6	186256	corn	Hajdúböszörmény, Hungary	104	coi-H4 (9)	28S-H6 (1)
7	184190	corn	Bonyhad, Tolna, Hungary	75	coi-H3 (8)	28S-H5 (1)
					coi-H7 (1)	
8	197260	corn	Bonyhad, Tolna, Hungary	62	coi-H3 (1)	-
9	197156	corn	Létavertes, Hajdú-Bihar, Hungary	480	coi-H10 (2)	28S-H8 (1)
10	197349	corn	Bagamer, Hajdú-Bihar, Hungary	629	coi-H3 (1)	28S-H4 (1)
					coi-H7 (1)	
					coi-H11 (1)	
11	197979	corn	Kondoros, Békés, Hungary	14	coi-H16 (5)	28S-H8 (2)
12	172745	wheat	Peregu Mare, Romania	620	-	28S-H9 (1)
13	185614	corn	Asola, Mantova, Italy	280	coi-H7 (1)	28S-H5 (1)
14	185343	corn	Roccabianca, Parma, Italy	479	coi-H3 (1)	28S-H5 (1)
15	185721	corn	Moretta, Cuneo, Italy	1760	coi-H3 (2)	28S-H5 (1)
					coi-H7 (7)	
16	ANT04	olive	Ancona, Ancona, Italy	321	coi-H3 (9)	28S-H5 (1)
					coi-H7 (2)	
17	185719	corn	Gaden, Bavaria, Germany	38	coi-H7 (11)	28S-H5 (1)
18	197227	corn	Möckmühl, Heilbronn, Germany	344	coi-H3 (1)	-
19	185601	corn	St. Padron de Conques, Aveyron, France.	4	coi-H3 (1)	28S-H5 (1)
20	186293	corn	Laurac, Languedoc-Rosellón, France	5	coi-H3 (1)	28S-H5 (1)
21	185733	corn	Neyron, Auvergne-Rhône-Alpes, France	22	coi-H3 (1)	28S-H5 (1)
22	184392	corn	Le Sen, Landes, France	313	coi-H3 (8)	28S-H5 (1)
23	172687	pea	Santarem, Santarem, Portugal	36	coi-H9(1)	28S-H7 (1)
24	184525	wheat	Bzenec, Moravia, Czech Republic	38	coi-H7 (7)	28S-H5 (1)
25	OLI087	olive	Istro, Crete, Greece	3	coi-H8 (8)	28S-H2 (2)
26	OLI038	olive	Hersonisos, Crete, Greece	13	coi-H1 (10)	28S-H1 (2)
27	OLI040	olive	Hersonisos, Crete, Greece	3	coi-H1 (11)	28S-H1 (1)
28	OlLI117	olive	Limnes, Crete, Greece	3	coi-H1 (9)	28S-H1 (2)

29	OLI119	olive	Limnes, Crete, Greece	8	coi-H1 (13)	28S-H1 (1)
30	ST079	olive	Huevar del Aljarafe, Sevilla, Spain	28	coi-H2(10)	28S-H3 (2)
31	J096	olive	Jerez de la Frontera, Cádiz, Spain	175	coi-H3(8)	28S-H5 (3)
32	AVER	hazelnut	Reus, Tarragona, Spain	24	coi-H3(7) coi-H13(3)	28S-H4 (1)
33	BAET	wild olive	Vejer de la Frontera, Cádiz, Spain	3	coi-H3(1)	28S-H5 (2)
34	ZARA	almond x peach	Montañana, Zaragoza, Spain	620	coi-H3(3)	-
35	185586	corn	Grenade, Haute-Garonne, France	21	coi-H3 (1)	28S-H5 (1)
36	197691	wheat	Mihail Kogalniceau, Romania	1711	coi-H11 (10)	-
37	197352	corn	Tépe, Hajdú-Bihar, Hungary	26	coi-H12 (2)	28S-H11 (2)

[a] coxI haplotype accessions: MT075822 (coi-H1); MT075823 (coi-H2); MT075824 (coi-H3); MT075825 (coi-H4); MT075826 (coi-H5); MT075827 (coi-H6); MT075828 (coi-H7); MT075829 (coi-H8); MT075830 (coi-H9); MT075831 (coi-H10); MT075832 (coi-H11); MT075833 (coi-H12); MT075834 (coi-H13); MT075835 (coi-H14); MT075836 (coi-H15); MT075837 (coi-H16). Number between parentheses indicate individuals detected in each haplotype.

[b] 28S haplotype accessions: MT084013 (28S-H1); MT084014 (28S-H2); MT084015 ((28S-H3); MT084016 (28S-H4); MT084017 (28S-H5); MT084018 (28S-H6); MT084019 (28S-H7); MT084020 (28S-H8); MT084021 (28S-H9); MT084022 (28S-H10); MT084023 (28S-H11); MT084024 (28S-H12); MT084025 (28S-H13). Number between parentheses indicate individuals detected in each haplotype.

TABLE 2. The frequency of the different *coxI* haplotypes of *Rotylenchulus macrosoma* found in different countries in Europe. Only those populations with ≥ 3 individuals sequenced are included[a].

	coi-H1	**coi-H2**	**coi-H3**	**coi-H4**	**coi-H5**	**coi-H6**	**coi-H7**	**coi-H8**	**coi-H9**	**coi-H10**	**coi-H11**	**coi-H12**	**coi-H13**	**coi-H14**	**coi-H15**	**coi-H16**	**n**	**Pop[b]**	***h*[c]**	***π***
Portugal									1								1	1	-	-
Spain		10	19										3				32	5 (1)	0,568 ± 0,063	0,032 ± 0,005
France			12														12	5 (4)	0,000 ± 0,000	0,000 ± 0,000
Italy			12				10										22	4 (2)	0,515 ± 0,052	0,011 ± 0,001
Germany			1				11										12	2 (1)	0,000 ± 0,000	0,000 ± 0,000
Hungary			10	9			2			2	1	2				5	31	7(1)	0.818 ± 0.039	0.035 ± 0.003
Czech Republic							7										7	1	0,000 ± 0,000	0,000 ± 0,000
Romania					3	2					20						25	3	0.353 ± 0.112	0,006 ± 0.002
Serbia			9	1										5	3		18	3 (1)	0,640 ± 0,080	0,034 ± 0,003
Crete, Greece	43							7									50	5	0,0219 ± 0,071	0,004 ± 0,001
Total	43	10	63	10	3	2	30	7	1	2	21	2	3	5	3	5	210			

[a] The total number of specimens, populations (Pop), the haplotype diversity h and nucleotide diversity π per country are stated
[b] Between parenthesis populations with only one individual sequenced because no other available individuals
[c] *h* = haplotype diversity; *π* = nucleotide diversity

TABLE 3. Pairwise F_{ST} values based on the *coxI* gene sequence of *Rotylenchulus macrosoma* samples from populations grouped by country of origin in Europe

	Spain	France	Italy	Germany	Hungary	Romania	Czech Republic	Serbia	Greece
Spain	-								
France	0.16774	-							
Italy	0.22701*[a]	0.30763	-						
Germany	0.43497*	1.00000*	0.44924*	-					
Hungary	0.24829*	0.33585*	0.28005*	0.33733*	-				
Romania	0.65936*	0.92049*	0.85808*	0.92274*	0.45543*	-			
Czech Republic	0.39784*	1.00000*	0.40029*	0.00000	0.30012*	0.91307*	-		
Serbia	0.20877*	0.31067	0.33748*	0.49094*	0.01381	0.51145*	0.43774*	-	
Crete, Greece	0.88051*	0.96983*	0.95101*	0.96898*	0.87190*	0.96157*	0.96681*	0.90624*	-

[a] Comparisons were significant between the two pairs of countries ($P < 0.01$) indicating significant genetic differentiation

TABLE 4. Results of a hierarchical AMOVA of populations of *Rotylenchulus macrosoma* based on the sequence of the *coxI* gene. The analysis is based on samples from 23 populations each one with at least 3 individuals sequenced and 9 countries.

Source of variation[3]	**d. f.**	**Sum of squares**	**Variance components**	**% of variation**		***P***
All sequences						
Among populations	22	2387.5	12.745 (Va)	97.47		
Within populations	173	57.2	0.330 (Vb)	2.53		
Fixation Indices						
F_{ST} (within populations)	0.975				Va and F_{ST}	< 0.0001[c]
Countries[a]						
Among countries	8	1926.1	9.862 (Va)	69.71		
Among populations within countries	14	461.5	3.954 (Vb)	27.95		
Within populations	173	57.2	0.330 (Vc)	2.34		
Fixation Indices						
F_{CT} (among countries)	0.697				Va and F_{CT}	< 0.0001[d]
F_{SC} (among populations within countries)	0.923				Vb and F_{SC}	< 0.0001[e]
F_{ST} (within populations)	0.977				Vc and F_{ST}	< 0.0001[c]
Europe (Western *vs* Eastern countries)[b]						
Among groups	1	444.8	3.809 (Va)	25.31		
Among populations within groups	21	1942.7	10.909 (Vb)	72.49		
Within populations	173	57.2	0.330 (Vc)	2.20		
Fixation Indices						
F_{CT} (among groups)	0.253				Va and F_{CT}	0.0196[d]
F_{SC} (among populations within groups)	0.971				Vb and F_{SC}	< 0.0001[e]
F_{ST} (within populations)	0.978				Vc and F_{ST}	< 0.0001[c]

[a] Countries: Spain, France, Germany, Italy, Czech Republic, Romania, Serbia, Hungary and Crete, Greece.
[b] Countries: Spain, France, Germany and Italy *vs*. Czech Republic, Romania, Serbia, Hungary, and Crete, Greece
[c] Probability of obtaining equal or lower F value determined by 1,023 randomizations by permuting haplotypes among populations among countries or groups.
[d] Probability of obtaining equal or lower F value determined by 1,023 randomizations by permuting populations among countries or groups.
[e] Probability of obtaining equal or lower F value determined by 1,023 randomizations by permuting haplotypes among populations within countries or groups.

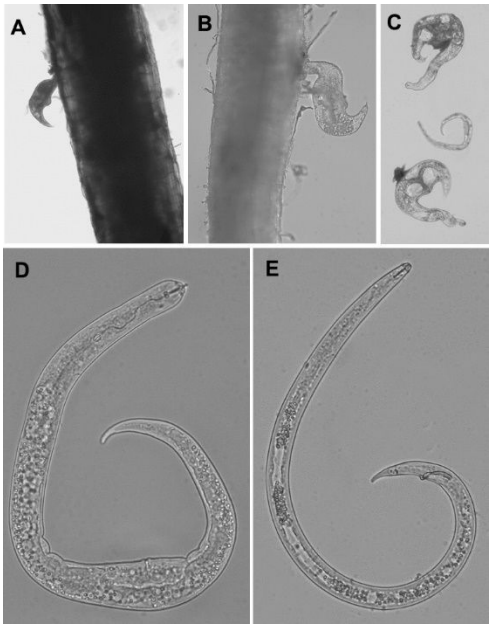
A
B
C
D
E

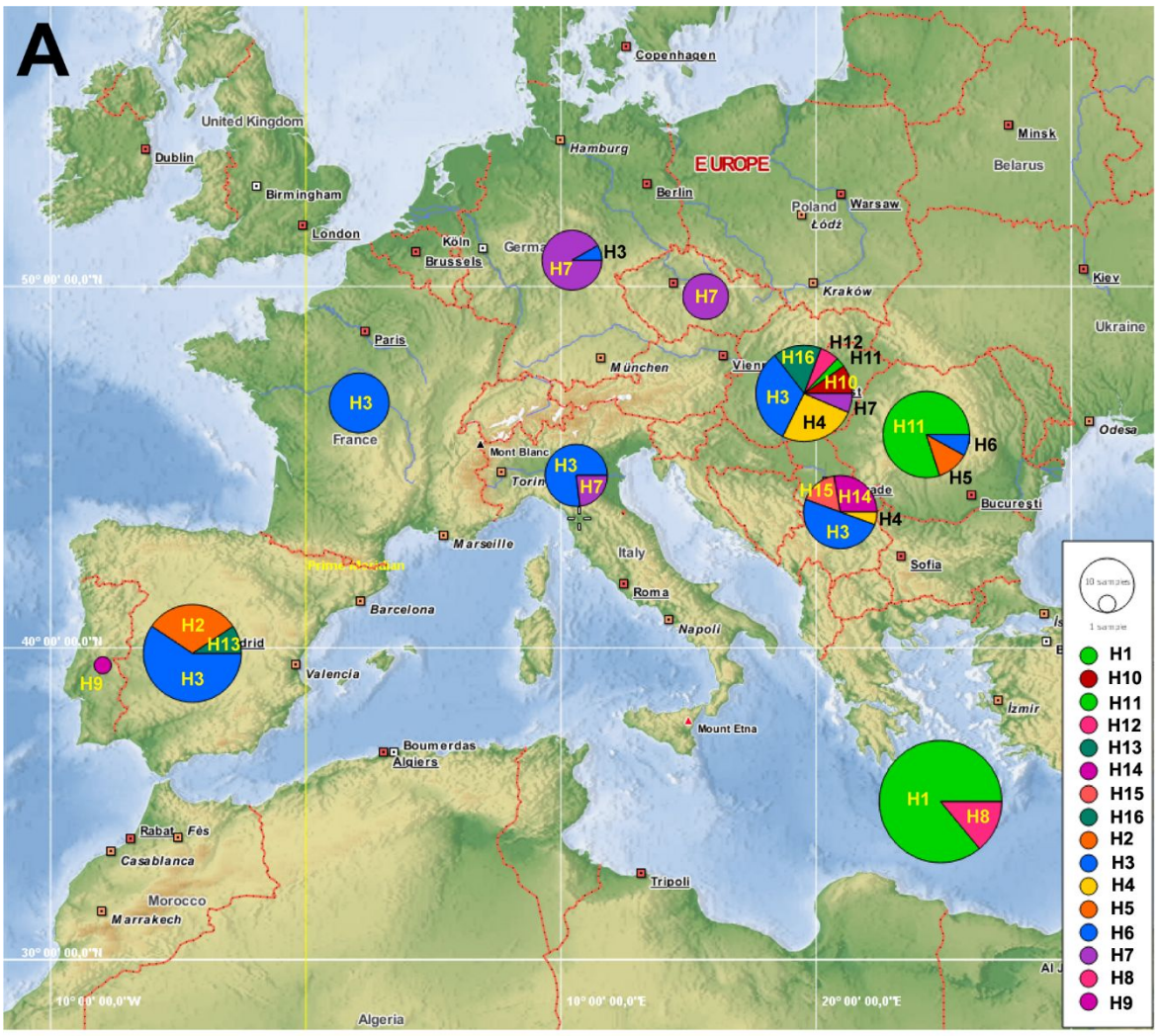
A
EUROPE
United Kingdom
Dublin
Birmingham
London
Copenhagen
Hamburg
Berlin
Köln
Brussels
Paris
München
Wien
Poland
Warsaw
Łódź
Kraków
Minsk
Belarus
Kiev
Ukraine
Odesa
Bucureşti
Sofia
Mont Blanc
Torino
Marseille
Italy
Roma
Napoli
Barcelona
Valencia
Madrid
Mount Etna
Izmir
Boumerdas
Algiers
Rabat
Fès
Casablanca
Morocco
Marrakech
Tripoli
Algeria
France
H1
H2
H3
H4
H5
H6
H7
H8
H9
H10
H11
H12
H13
H14
H15
H16

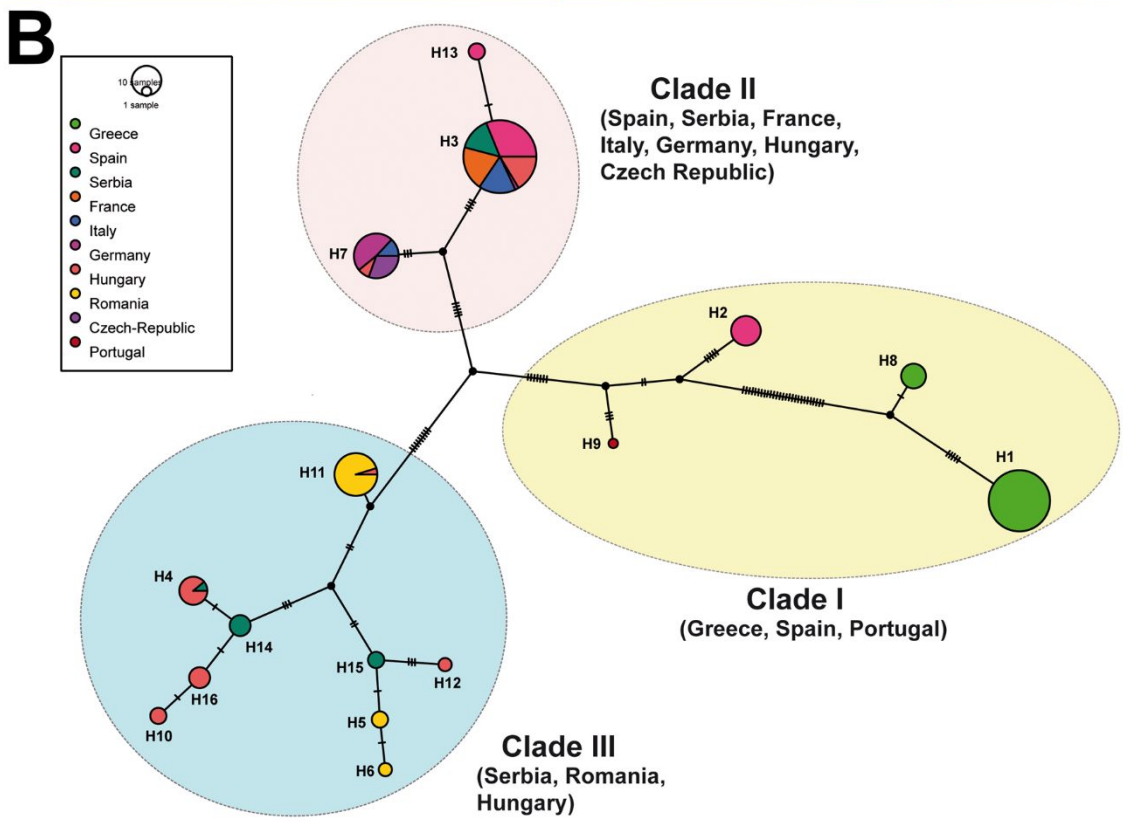
B
10 samples
1 sample
Greece
Spain
Serbia
France
Italy
Germany
Hungary
Romania
Czech-Republic
Portugal
Clade II
(Spain, Serbia, France, Italy, Germany, Hungary, Czech Republic)
Clade I
(Greece, Spain, Portugal)
Clade III
(Serbia, Romania, Hungary)
H1
H2
H3
H4
H5
H6
H7
H8
H9
H10
H11
H12
H13
H14
H15
H16

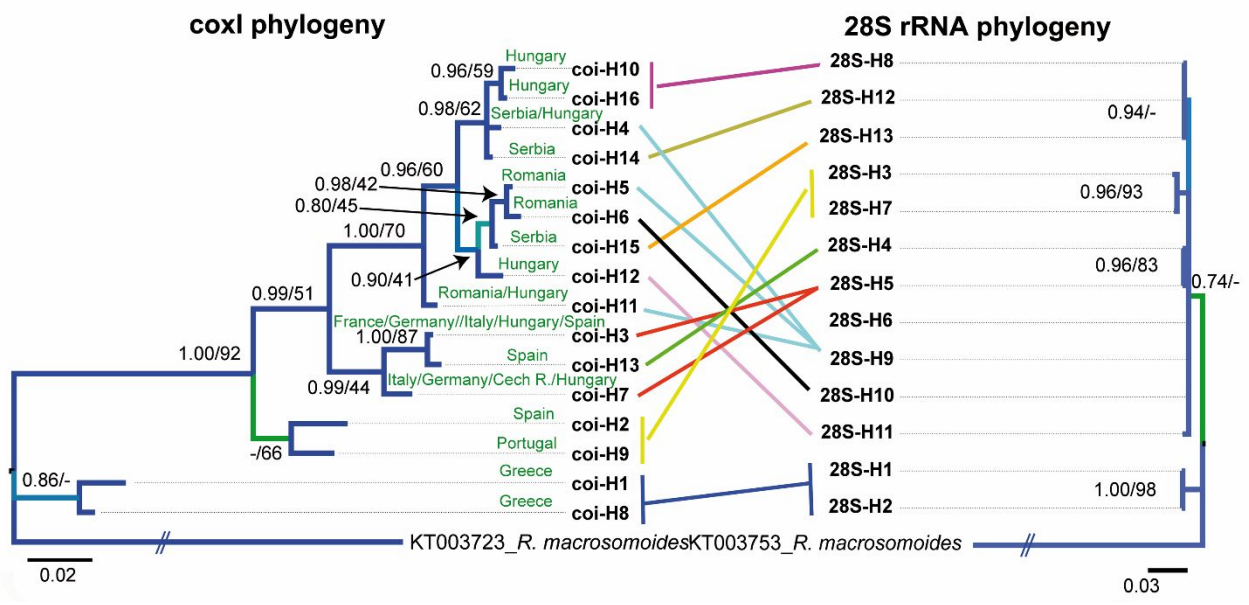
coxI phylogeny
28S rRNA phylogeny
Hungary
Hungary
Serbia/Hungary
Serbia
Romania
Romania
Serbia
Hungary
Romania/Hungary
France/Germany//Italy/Hungary/Spain
Spain
Italy/Germany/Cech R./Hungary
Spain
Portugal
Greece
Greece
coi-H10
coi-H16
coi-H4
coi-H14
coi-H5
coi-H6
coi-H15
coi-H12
coi-H11
coi-H3
coi-H13
coi-H7
coi-H2
coi-H9
coi-H1
coi-H8
28S-H8
28S-H12
28S-H13
28S-H3
28S-H7
28S-H4
28S-H5
28S-H6
28S-H9
28S-H10
28S-H11
28S-H1
28S-H2
0.96/59
0.98/62
0.96/60
0.98/42
0.80/45
1.00/70
0.90/41
0.99/51
1.00/87
1.00/92
0.99/44
-/66
0.86/-
0.94/-
0.96/93
0.96/83
0.74/-
1.00/98
KT003723_R. macrosomoidesKT003753_R. macrosomoides
0.02
0.03

Supplementary tables

Table S1. Tajima-D and Fu-Fs tests for populations.

Table S2. Comparison of pairs of population for the Fst.

Table S3. Tajima-D and Fu-Fs tests for country.

Supplementary Figs

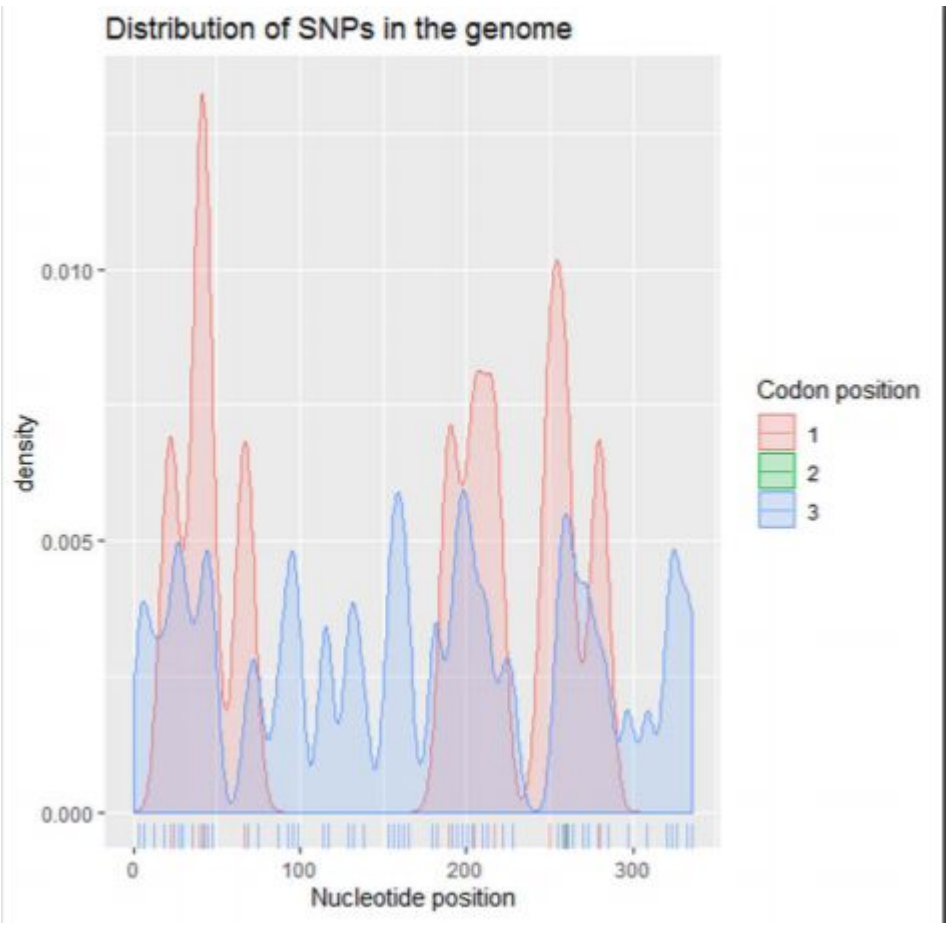

```
                    10        20        30        40        50        60        70        80        90
           ....|....|....|....|....|....|....|....|....|....|....|....|....|....|....|....|....|....|
coi-H1     NKNIFGNLGMI*ALVSIGFIGCLVWAHHIFVVGIDLDSRAYFSAATIIIAVPTGVNVFSWMITLYGIYFFYNPLFLWINGFIFLFTVGGL
coi-H2     .N.......I.Y..........M.....................................I...........S.............T...
coi-H3     .N.......I.Y..I.......I.....................................I.......I...S.............T...
coi-H4     .N.......I.Y..........M.....M...............................I......*I...S.............T...
coi-H5     KN.......I.Y..........I.....M...............................I.......I...S.............T...
coi-H6     KN.......I.Y..........I.....M...............................I.......I...S.............T...
coi-H7     .N.......I.Y..........I.....................................I.......I...S.............T...
coi-H8     ...........Y.......................................................................
coi-H9     .N.......I.Y..........I.....................................I...........S.............T...
coi-H10    .N.......I.Y..........I.....M...............................I......*I...S.............T...
coi-H11    KN.......I.Y..........I.....M...............................I......*I...S.............T...
coi-H12    KN.......I.Y..........I.....M...............................I......*I...S.............T...
coi-H13    .N.......I.Y..I.......I.....................................I.......I...S.............T...
coi-H14    .N.......I.Y..........I.....M...............................I......*I...S.............T...
coi-H15    KN.......I.Y..........I.....M...............................I......*I...S.............T...
coi-H16    .N.......I.Y..........I.....M...............................I......*I...S.............T...

                    110
           ....|....|.
coi-H1     DLLLHDTYYVV
coi-H2     ...........
coi-H3     ...........
coi-H4     ...........
coi-H5     ...........
coi-H6     ...........
coi-H7     ...........
coi-H8     ...........
coi-H9     ........*..
coi-H10    ...........
coi-H11    ...........
coi-H12    ...........
coi-H13    ...........
coi-H14    ...........
coi-H15    ...........
coi-H16    ...........
```

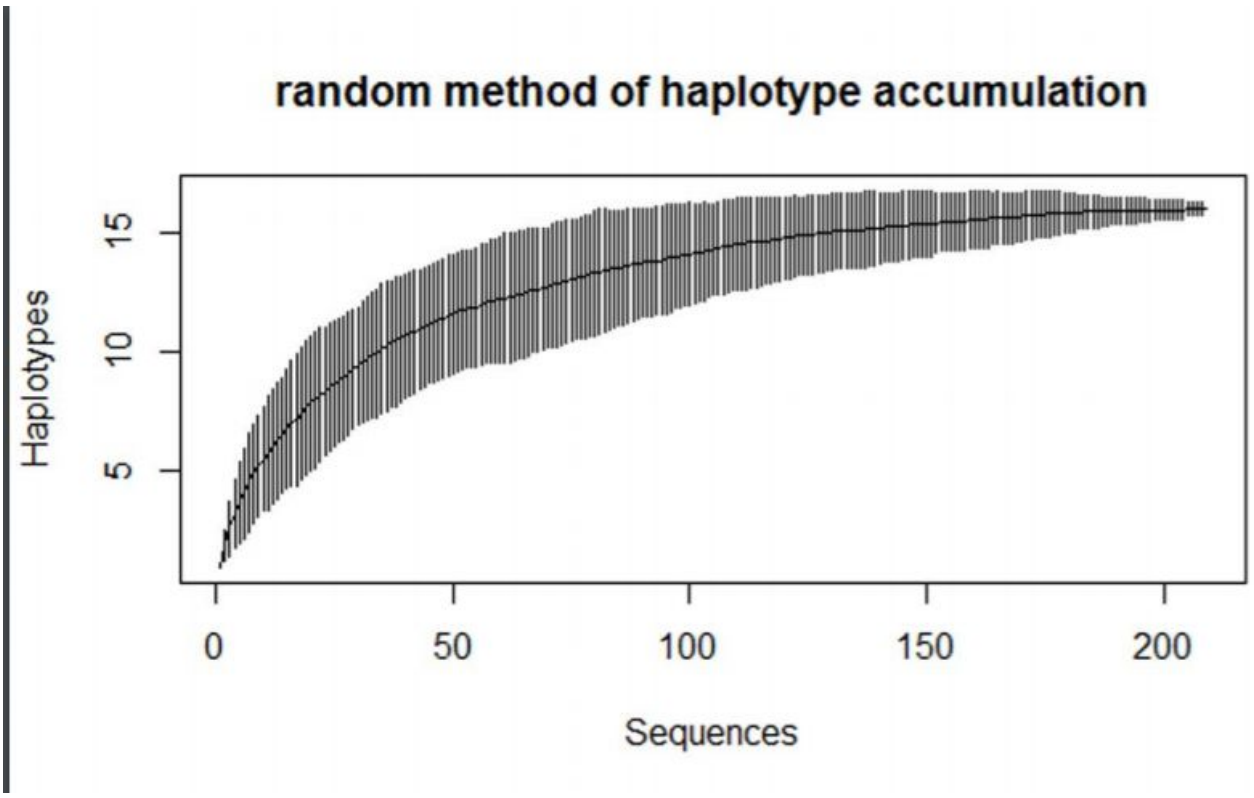
random method of haplotype accumulation
Haplotypes
5
10
15
0
50
100
150
200
Sequences

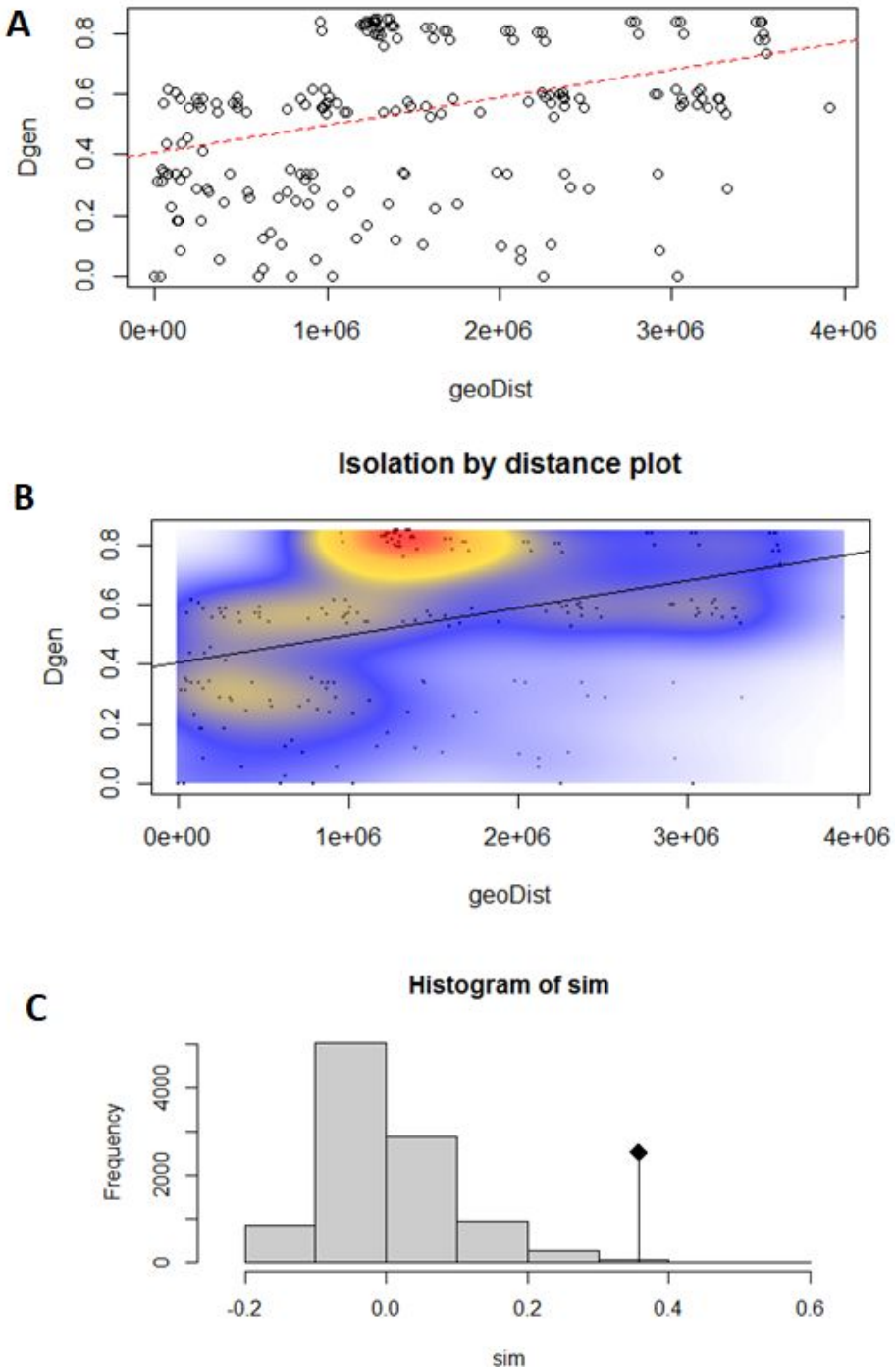
A
Dgen
0.0
0.2
0.4
0.6
0.8
0e+00
1e+06
2e+06
3e+06
4e+06
geoDist
Isolation by distance plot
B
Dgen
0.0
0.2
0.4
0.6
0.8
0e+00
1e+06
2e+06
3e+06
4e+06
geoDist
Histogram of sim
C
Frequency
0
2000
4000
-0.2
0.0
0.2
0.4
0.6
sim

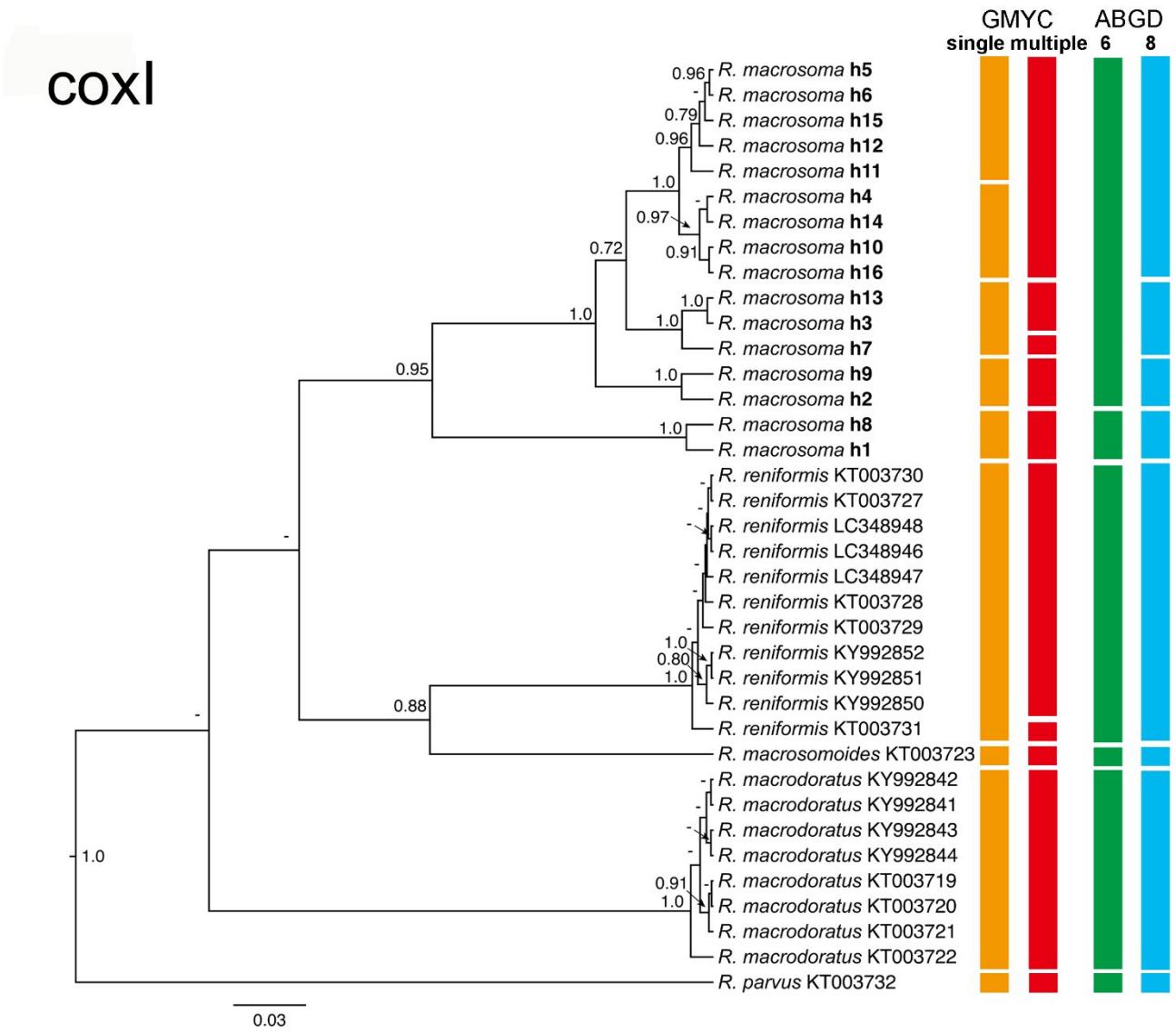
coxI
GMYC
single multiple
ABGD
6
8
R. macrosoma h5
R. macrosoma h6
R. macrosoma h15
R. macrosoma h12
R. macrosoma h11
R. macrosoma h4
R. macrosoma h14
R. macrosoma h10
R. macrosoma h16
R. macrosoma h13
R. macrosoma h3
R. macrosoma h7
R. macrosoma h9
R. macrosoma h2
R. macrosoma h8
R. macrosoma h1
R. reniformis KT003730
R. reniformis KT003727
R. reniformis LC348948
R. reniformis LC348946
R. reniformis LC348947
R. reniformis KT003728
R. reniformis KT003729
R. reniformis KY992852
R. reniformis KY992851
R. reniformis KY992850
R. reniformis KT003731
R. macrosomoides KT003723
R. macrodoratus KY992842
R. macrodoratus KY992841
R. macrodoratus KY992843
R. macrodoratus KY992844
R. macrodoratus KT003719
R. macrodoratus KT003720
R. macrodoratus KT003721
R. macrodoratus KT003722
R. parvus KT003732
0.03

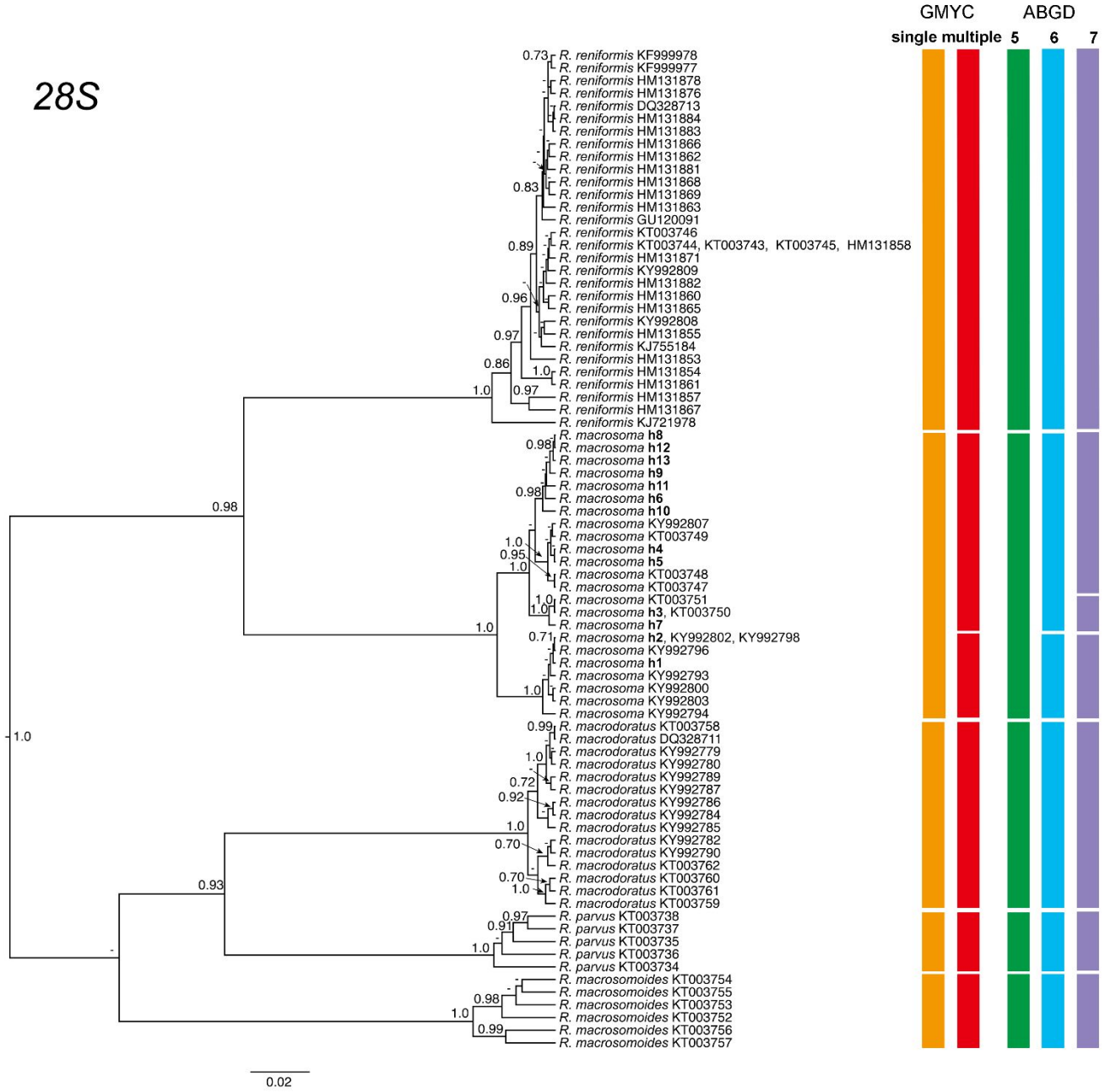
28S
GMYC
ABGD
single multiple 5 6 7
R. reniformis KF999978
R. reniformis KF999977
R. reniformis HM131878
R. reniformis HM131876
R. reniformis DQ328713
R. reniformis HM131884
R. reniformis HM131883
R. reniformis HM131866
R. reniformis HM131862
R. reniformis HM131881
R. reniformis HM131868
R. reniformis HM131869
R. reniformis HM131863
R. reniformis GU120091
R. reniformis KT003746
R. reniformis KT003744, KT003743, KT003745, HM131858
R. reniformis HM131871
R. reniformis KY992809
R. reniformis HM131882
R. reniformis HM131860
R. reniformis HM131865
R. reniformis KY992808
R. reniformis HM131855
R. reniformis KJ755184
R. reniformis HM131853
R. reniformis HM131854
R. reniformis HM131861
R. reniformis HM131857
R. reniformis HM131867
R. reniformis KJ721978
R. macrosoma h8
R. macrosoma h12
R. macrosoma h13
R. macrosoma h9
R. macrosoma h11
R. macrosoma h6
R. macrosoma h10
R. macrosoma KY992807
R. macrosoma KT003749
R. macrosoma h4
R. macrosoma h5
R. macrosoma KT003748
R. macrosoma KT003747
R. macrosoma KT003751
R. macrosoma h3, KT003750
R. macrosoma h7
R. macrosoma h2, KY992802, KY992798
R. macrosoma KY992796
R. macrosoma h1
R. macrosoma KY992793
R. macrosoma KY992800
R. macrosoma KY992803
R. macrosoma KY992794
R. macrodoratus KT003758
R. macrodoratus DQ328711
R. macrodoratus KY992779
R. macrodoratus KY992780
R. macrodoratus KY992789
R. macrodoratus KY992787
R. macrodoratus KY992786
R. macrodoratus KY992784
R. macrodoratus KY992785
R. macrodoratus KY992782
R. macrodoratus KY992790
R. macrodoratus KT003762
R. macrodoratus KT003760
R. macrodoratus KT003761
R. macrodoratus KT003759
R. parvus KT003738
R. parvus KT003737
R. parvus KT003735
R. parvus KT003736
R. parvus KT003734
R. macrosomoides KT003754
R. macrosomoides KT003755
R. macrosomoides KT003753
R. macrosomoides KT003752
R. macrosomoides KT003756
R. macrosomoides KT003757
0.02

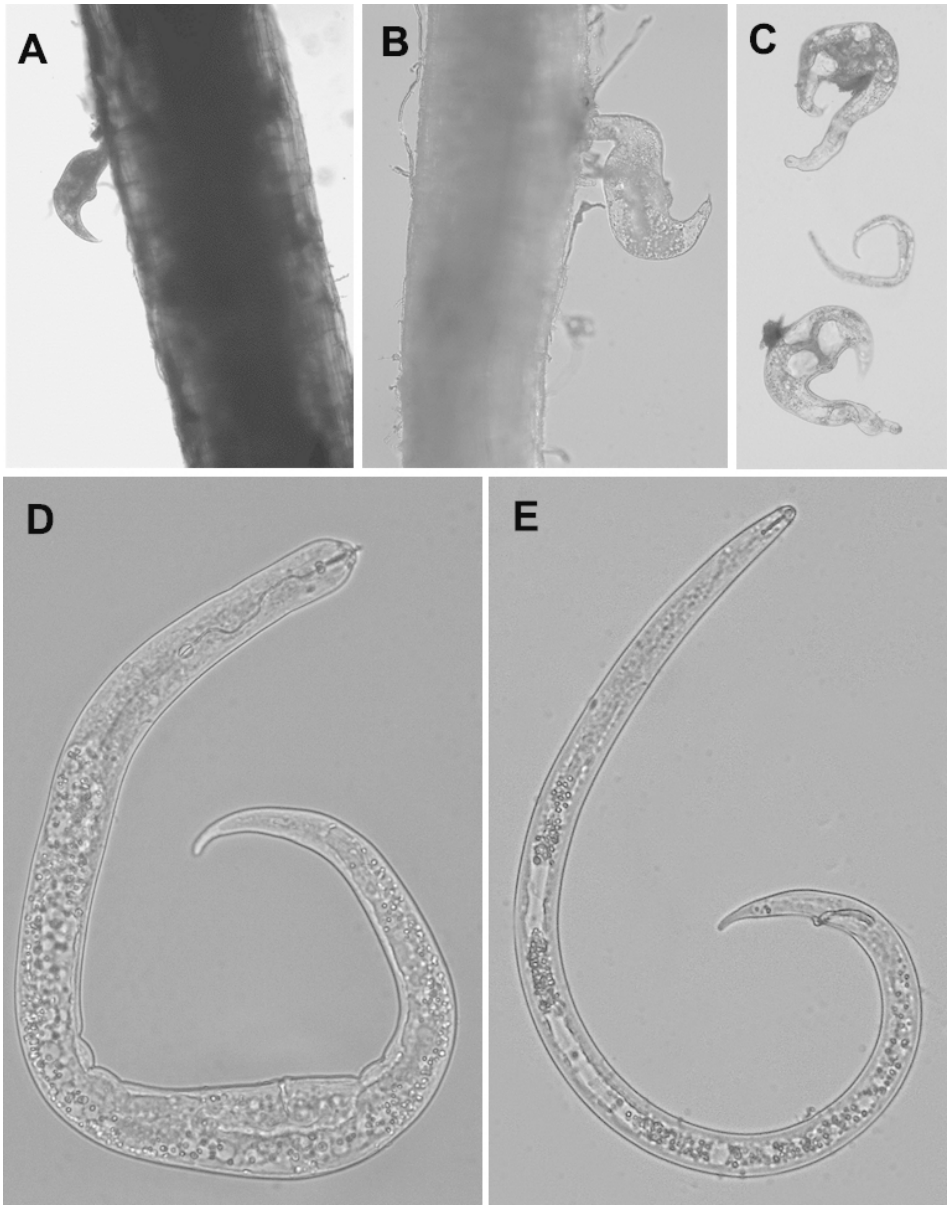

Figure 1

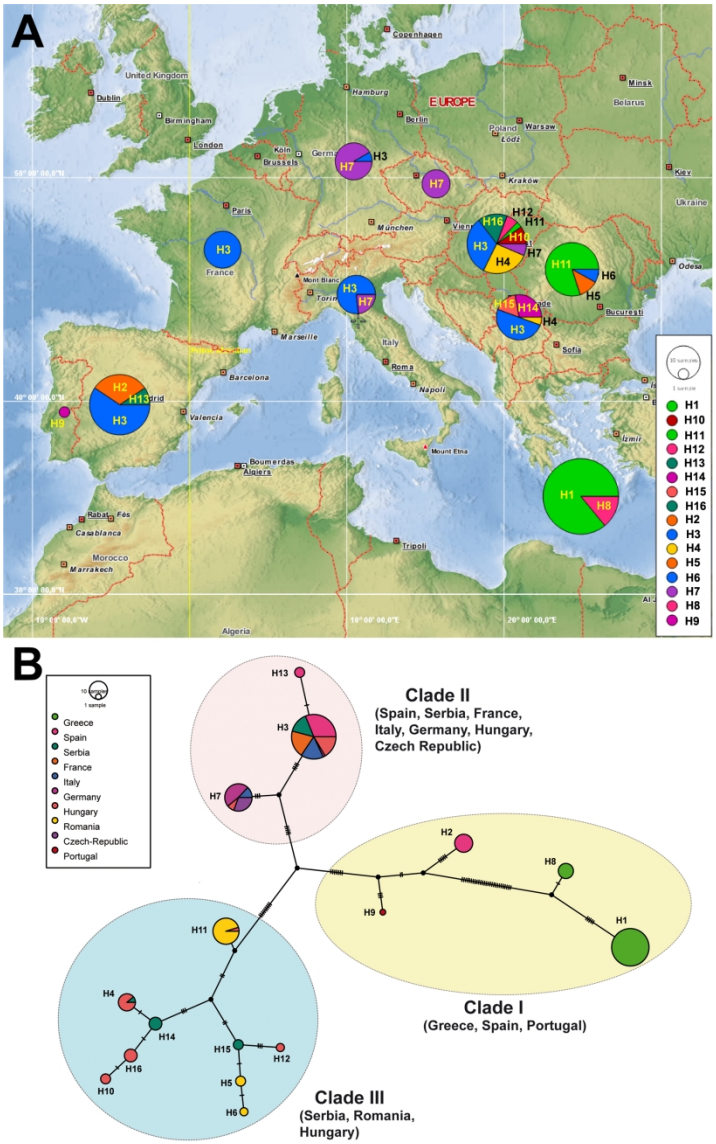
A
EUROPE
H1
H10
H11
H12
H13
H14
H15
H16
H2
H3
H4
H5
H6
H7
H8
H9
B
Greece
Spain
Serbia
France
Italy
Germany
Hungary
Romania
Czech-Republic
Portugal
Clade II
(Spain, Serbia, France, Italy, Germany, Hungary, Czech Republic)
Clade I
(Greece, Spain, Portugal)
Clade III
(Serbia, Romania, Hungary)

Figure 2

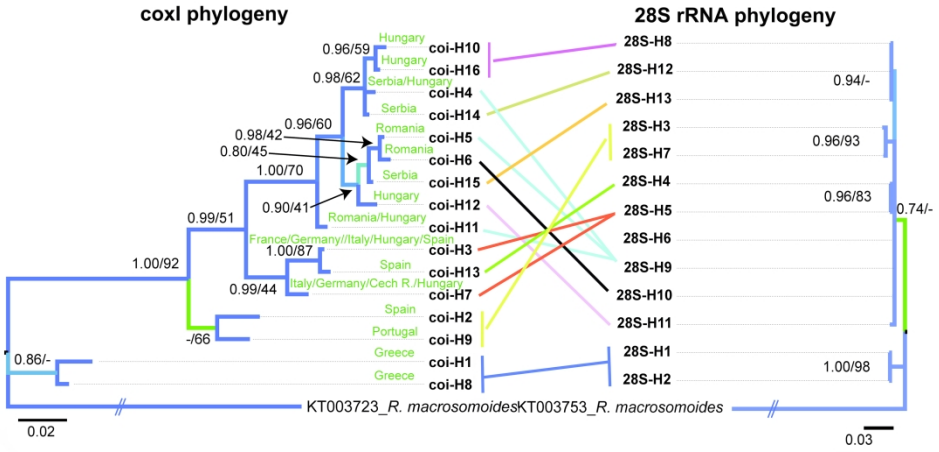
coxI phylogeny
28S rRNA phylogeny
0.96/59
0.98/62
0.96/60
0.98/42
0.80/45
1.00/70
0.90/41
0.99/51
1.00/92
1.00/87
0.99/44
-/66
0.86/-
Hungary
Hungary
Serbia/Hungary
Serbia
Romania
Romania
Serbia
Hungary
Romania/Hungary
France/Germany//Italy/Hungary/Spain
Spain
Italy/Germany/Cech R./Hungary
Spain
Portugal
Greece
Greece
coi-H10
coi-H16
coi-H4
coi-H14
coi-H5
coi-H6
coi-H15
coi-H12
coi-H11
coi-H3
coi-H13
coi-H7
coi-H2
coi-H9
coi-H1
coi-H8
28S-H8
28S-H12
28S-H13
28S-H3
28S-H7
28S-H4
28S-H5
28S-H6
28S-H9
28S-H10
28S-H11
28S-H1
28S-H2
0.94/-
0.96/93
0.96/83
0.74/-
1.00/98
KT003723_R. macrosomoides
KT003753_R. macrosomoides
0.02
0.03

Figure 3

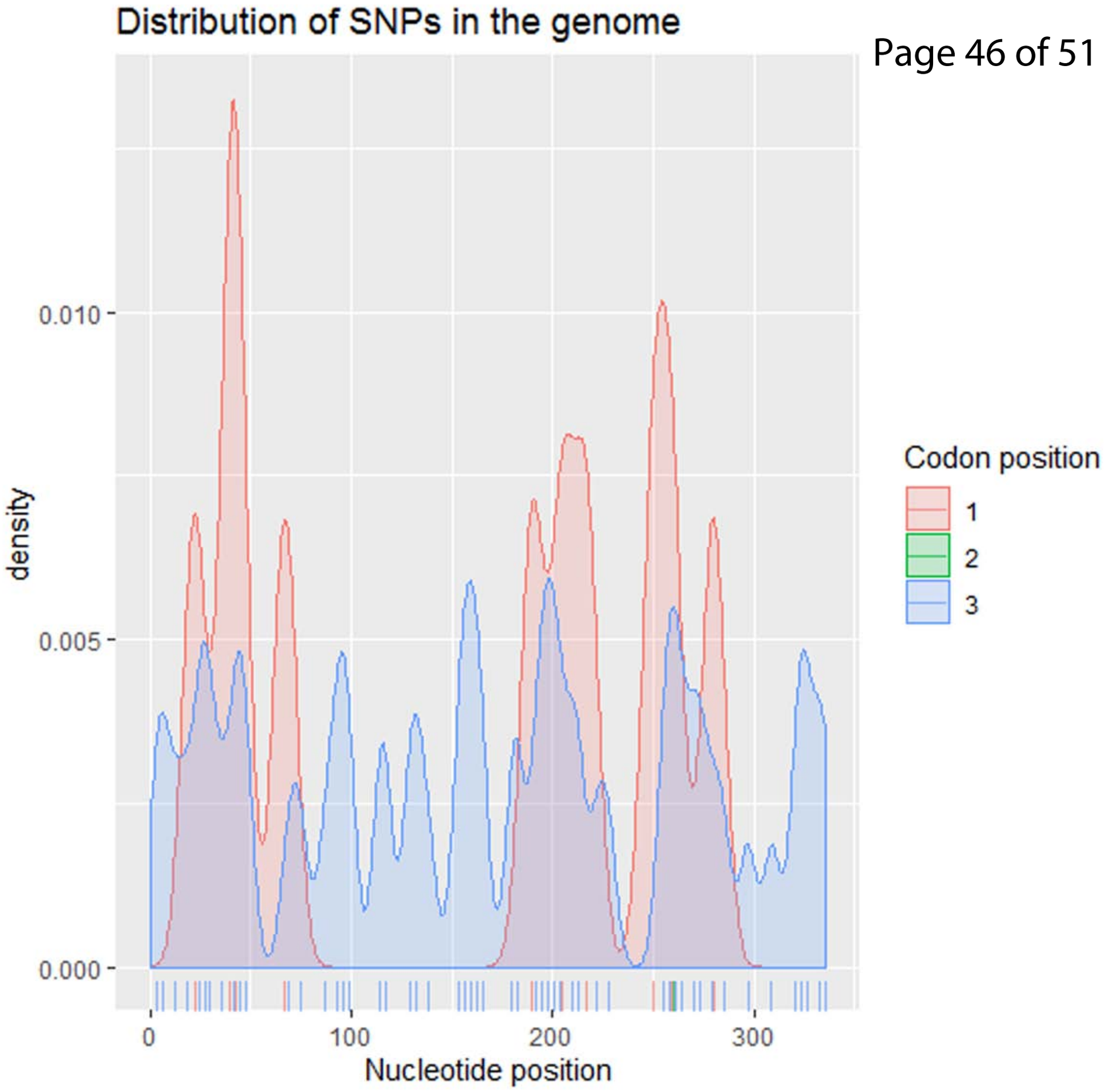
Distribution of SNPs in the genome
density
0.010
0.005
0.000
0
100
200
300
Nucleotide position
Codon position
1
2
3

```
                    10        20        30        40        50        60        70        80        90
          1 . . |....|....|....|....|....|....|....|....|....|....|....|....|....|....|....|....|....|....|
coi-H1    NKNIFGNLGMI*ALVSIGFIGCLVWAHHIFVVGIDLDSRAYFSAATIIIAVPTGVNVFSWMITLYGIYFFYNPLFLWINGFIFLFTVGGL
coi-H2    .N.......I.Y..........M.......................................I...........S.............T...
coi-H3    .N.......I.Y..I.......I.......................................I.......I...S.............T...
coi-H4    .N.......I.Y..........M.....M.................................I......*I...S.............T...
coi-H5    KN.......I.Y..........I.....M.................................I.......I...S.............T...
coi-H6    KN.......I.Y..........I.....M.................................I.......I...S.............T...
coi-H7    .N.......I.Y..........I.......................................I.......I...S.............T...
coi-H8    ...........Y..........................................................................
coi-H9    .N.......I.Y..........I.......................................I...........S.............T...
coi-H10   .N.......I.Y..........I.....M.................................I......*I...S.............T...
coi-H11   KN.......I.Y..........I.....M.................................I......*I...S.............T...
coi-H12   KN.......I.Y..........I.....M.................................I......*I...S.............T...
coi-H13   .N.......I.Y..I.......I.......................................I.......I...S.............T...
coi-H14   .N.......I.Y..........I.....M.................................I......*I...S.............T...
coi-H15   KN.......I.Y..........I.....M.................................I......*I...S.............T...
coi-H16   .N.......I.Y..........I.....M.................................I......*I...S.............T...

                    110
          ....|....|.
coi-H1    DLLLHDTYYVV
coi-H2    ...........
coi-H3    ...........
coi-H4    ...........
coi-H5    ...........
coi-H6    ...........
coi-H7    ...........
coi-H8    ...........
coi-H9    ........*..
coi-H10   ...........
coi-H11   ...........
coi-H12   ...........
coi-H13   ...........
coi-H14   ...........
coi-H15   ...........
coi-H16   ...........
```

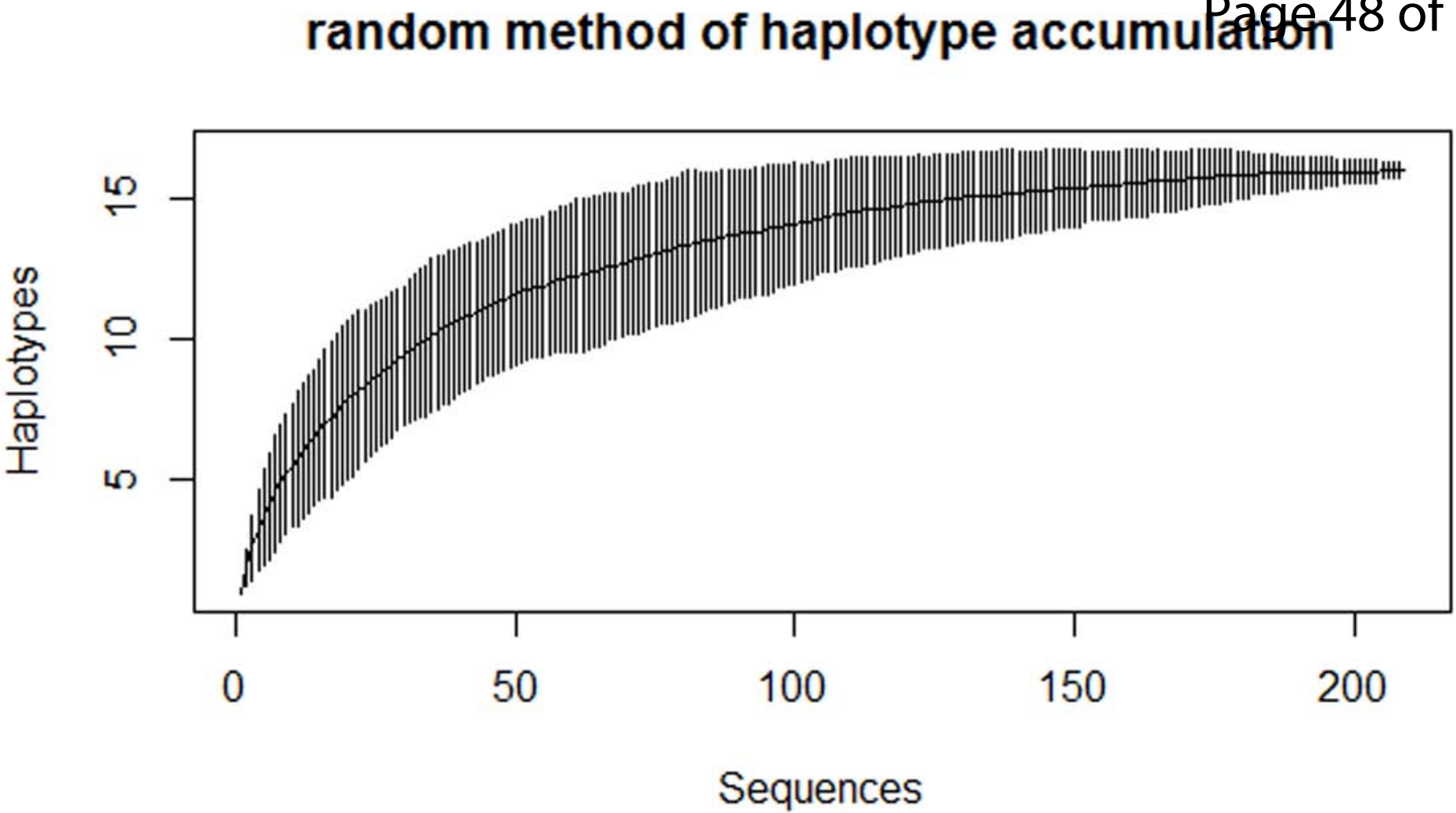
random method of haplotype accumulation
Haplotypes
5
10
15
0
50
100
150
200
Sequences

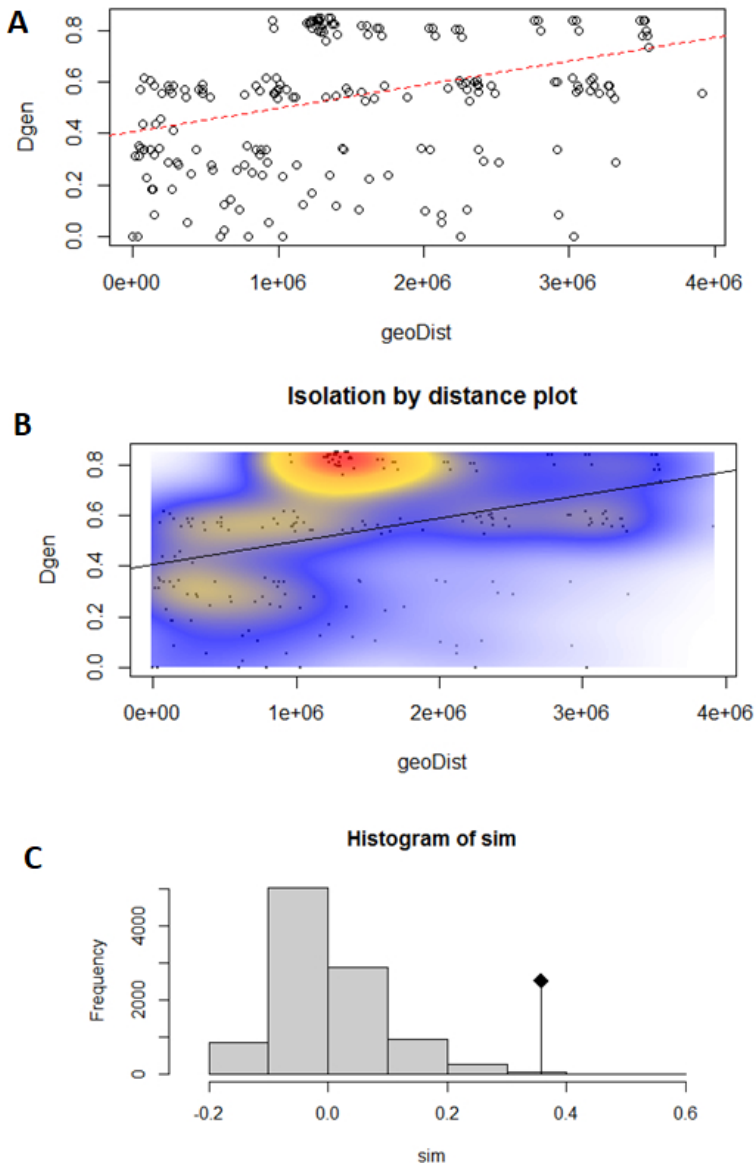

Fig.S4

27x41mm (500 x 500 DPI)

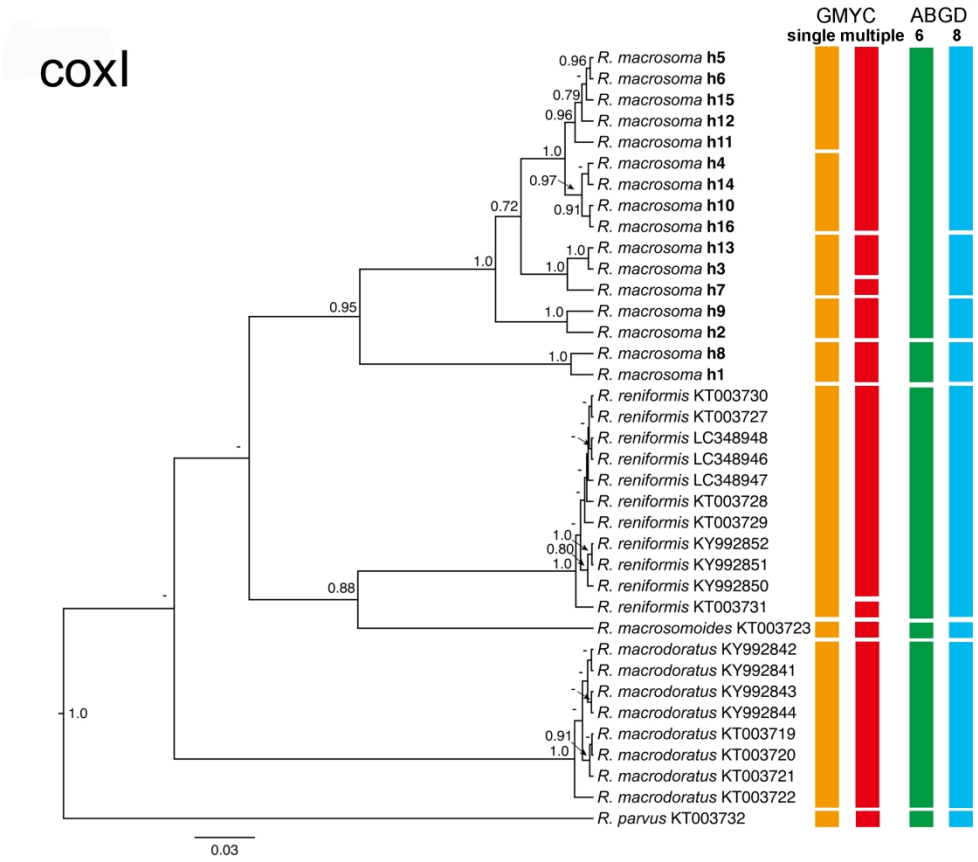
coxI
GMYC
single multiple
ABGD
6
8
R. macrosoma h5
R. macrosoma h6
R. macrosoma h15
R. macrosoma h12
R. macrosoma h11
R. macrosoma h4
R. macrosoma h14
R. macrosoma h10
R. macrosoma h16
R. macrosoma h13
R. macrosoma h3
R. macrosoma h7
R. macrosoma h9
R. macrosoma h2
R. macrosoma h8
R. macrosoma h1
R. reniformis KT003730
R. reniformis KT003727
R. reniformis LC348948
R. reniformis LC348946
R. reniformis LC348947
R. reniformis KT003728
R. reniformis KT003729
R. reniformis KY992852
R. reniformis KY992851
R. reniformis KY992850
R. reniformis KT003731
R. macrosomoides KT003723
R. macrodoratus KY992842
R. macrodoratus KY992841
R. macrodoratus KY992843
R. macrodoratus KY992844
R. macrodoratus KT003719
R. macrodoratus KT003720
R. macrodoratus KT003721
R. macrodoratus KT003722
R. parvus KT003732
0.03

Fig. S5

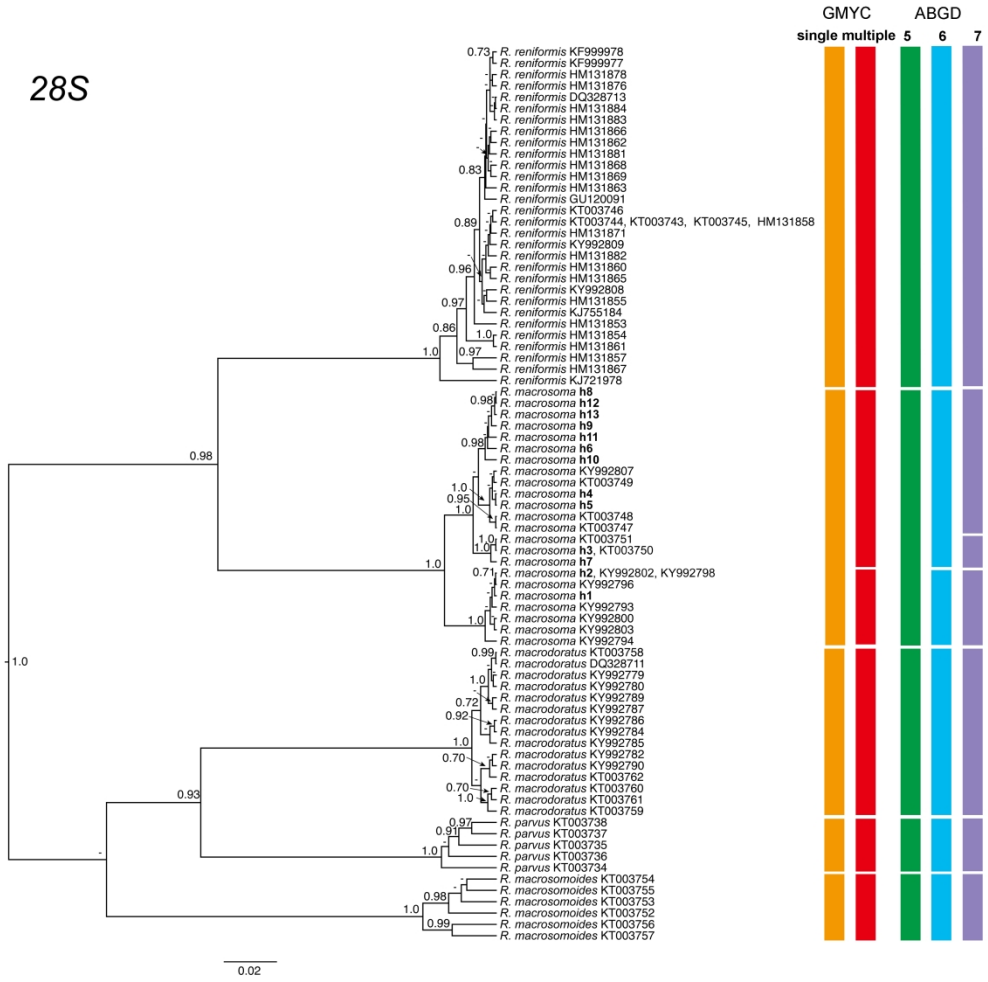
28S
GMYC
ABGD
single multiple 5 6 7
R. reniformis KF999978
R. reniformis KF999977
R. reniformis HM131878
R. reniformis HM131876
R. reniformis DQ328713
R. reniformis HM131884
R. reniformis HM131883
R. reniformis HM131866
R. reniformis HM131862
R. reniformis HM131881
R. reniformis HM131868
R. reniformis HM131869
R. reniformis HM131863
R. reniformis GU120091
R. reniformis KT003746
R. reniformis KT003744, KT003743, KT003745, HM131858
R. reniformis HM131871
R. reniformis KY992809
R. reniformis HM131882
R. reniformis HM131860
R. reniformis HM131865
R. reniformis KY992808
R. reniformis HM131855
R. reniformis KJ755184
R. reniformis HM131853
R. reniformis HM131854
R. reniformis HM131861
R. reniformis HM131857
R. reniformis HM131867
R. reniformis KJ721978
R. macrosoma h8
R. macrosoma h12
R. macrosoma h13
R. macrosoma h9
R. macrosoma h11
R. macrosoma h6
R. macrosoma h10
R. macrosoma KY992807
R. macrosoma KT003749
R. macrosoma h4
R. macrosoma h5
R. macrosoma KT003748
R. macrosoma KT003747
R. macrosoma KT003751
R. macrosoma h3, KT003750
R. macrosoma h7
R. macrosoma h2, KY992802, KY992798
R. macrosoma KY992796
R. macrosoma h1
R. macrosoma KY992793
R. macrosoma KY992800
R. macrosoma KY992803
R. macrosoma KY992794
R. macrodoratus KT003758
R. macrodoratus DQ328711
R. macrodoratus KY992779
R. macrodoratus KY992780
R. macrodoratus KY992789
R. macrodoratus KY992787
R. macrodoratus KY992786
R. macrodoratus KY992784
R. macrodoratus KY992785
R. macrodoratus KY992782
R. macrodoratus KY992790
R. macrodoratus KT003762
R. macrodoratus KT003760
R. macrodoratus KT003761
R. macrodoratus KT003759
R. parvus KT003738
R. parvus KT003737
R. parvus KT003735
R. parvus KT003736
R. parvus KT003734
R. macrosomoides KT003754
R. macrosomoides KT003755
R. macrosomoides KT003753
R. macrosomoides KT003752
R. macrosomoides KT003756
R. macrosomoides KT003757
0.02

Fig. S6